Horizontal Adaptive Optics in the Ground Layer Atmosphere

Nils Håkansson

Lund Observatory
Lund University

Horizontal Adaptive Optics in the Ground Layer Atmosphere

N. Håkansson

June 17, 2010

Lund Observatory, Lund University, Sweden
Supervisor: Torben Andersen
Co-supervisor: Mette Owner-Petersen

Abstract

The usual terrestrial optical astronomy is focused on observing vertically through the atmosphere. When traveling through the atmosphere, the light coming from distant objects gets distorted by the turbulent atmosphere due to varying refractive indices. The effects varies with time and causes position shifts, size changes and intensity variations in an image. The closer to the ground that the light travels, the more distorted the image gets. For this thesis, the atmosphere was studied horizontally and close to the ground, thus the image gets greatly distorted. Using an adaptive optics setup to observe several light reflecting objects and several luminous objects at varying distances, the atmosphere is characterized by two parameters, coherence length (r_0) and coherence time (τ_0). The image improvement by the system is also studied.

The atmospheric coherence length changes with distance, from an average of $r_0 \approx 5.1$ cm at 70 m to $r_0 \approx 3$ cm at 600 m. The system used works well at 70 meters if the coherence length is above about one or two centimeters, but at longer distances the system is not as successful. Several improvements to the system are finally suggested.

Summary in Swedish

Ljus som kommer från en extern källa och färdas genom jordens atmosfär blir förvrängt. Det mesta av förvrängningen (90%) sker i det lägsta lagret av atmosfären, det såkallade grundlagret (Ground Layer). Tjockleken på detta lager varierar mellan 100 och 1500 meter beroende på vart på jorden det är och hur högt över havsytan det är.

Normalt för markbaserad optisk astronomi är att studera object som befinner sig mer eller mindre vertikalt ovanför observatoriet. För att korrigera för atmosfärens turbulens används adaptiv optik (Adaptive Optics, AO). På grund av att det är grundlagret som skapar det mesta av distorsionen i atmosfären så har det inom astronomin bedrivits mycket forskning på hur atmosfären fungerar i grundlagret vertikalt för att få den adaptive optiken funktionell.

Horisontellt har atmosfären inte studerats alls lika noggrant som vertikalt. Horisontellt sträcker sig atmosfären sig längre än 1500 meter och därav blir ljus som kommer från längre avstånd att bli mer förvrängt än om det kommit vertikalt. Det kan vara av intresse att studera atmosfären horisontellt då det kan minska kraven som finns på teleskop, för astronomiskt bruk och för annat bruk, exempelvis laserkommunikation. Motivet för detta mastersprojekt, där jag arbetar med ett nytt koncept kallat "Horizontal Adaptive Optics in the Ground Layer Atmosphere" (HAOGLA).

Contents

Table 1: A list of abbreviations and acronyms.

Abbreviations and acronyms	Long form
AO	Adaptive Optics
CCD	Charge Coupled Device
r_0	Coherence length
τ_0	Coherence time
DM	Deformable Mirror
fft	fast Fourier transform
FoV	Field of View
HAOGLA	Horizontal Adaptive Optics in the Ground Layer Atmosphere
LED	Light Emitting Diode
Q.E	Quantum Efficiency
C_N^2	Refractive index structure parameter
SC	Science Camera
SVD	Singular Value Decomposition
STM	Sun Target Mirror
TT	tip-tilt
WFS	Wave Front Sensor

1   Introduction

Light coming from any source and traveling through the atmosphere gets distorted by the atmosphere. Most of the distortions (about 90%) occurs in the part of the atmosphere that is closest to the ground, the so called ground layer. This ground layer reaches from the ground up to between 100 and 1500 meters depending on several factors. Factors such as the geographical location, time of day and ground elevation above sea level.

In ground based astronomy the normal direction to look at targets is more or less vertically upwards, thus the light coming form some object, e.g. a star, has passed through the atmosphere and became distorted before it is collected. Adaptive optics (AO) is used to correct for the distortions created in the atmosphere. For the AO to work properly the atmosphere has been studied in great detail, but because it is the ground layer that causes the most distortions most of the focus has been directed towards correcting for this vertically. Ground layer C_N^2 gives the possibility to predict coherence lengths as a function of propagation distance. What is meant by C_N^2 and coherence length will be taken up in the report. How the atmosphere works when there is only ground layer atmosphere that distorts the light (e.g. horizontally) is not studied very much at all. This information will be useful in the future to confine constraints on telescopes and other areas outside of astronomy such as laser communication.

The aim of this master thesis is to get a greater understanding of how the ground layer atmosphere distorts light coming from some object in the horizontal plane. The focus is to see whether it is possible to do "Horizontal Adaptive Optics in the Ground Layer Atmosphere" (HAOGLA) in Lund.

After this introduction comes section 2 that has some background information about the subject as a whole. Section 3 handles the theory that is useful to this thesis with coherence length, coherence time, atmospheric profiles, image movement and flux calculations. In section 4 can be seen information about the equipment used and information about the targeted object (man made, since it is not a stellar object being targeted on Earth). The method used during this thesis work is explained in section 5. Section 6 is about the results and the conclusions of this thesis. A discussion of this thesis is in the final section, section 7.

There are two appendices to the thesis, the first contains all the plots that have been made for this thesis. The second appendix contains a manual on how to use the setup used for this thesis, how it should be calibrated and solutions to specific errors that occurs more often.

A final thing to point out is the list of abbreviations and acronyms in table 1.

2   Background

As stated in the previous section, the atmosphere distorts incoming light that is used to study some object or the medium in between the telescope and the object. In order to compensate for the atmosphere there is a need to classify the atmosphere with some parameters.

There are three primary parameters used to classify the atmosphere, the coherence length, r_0, the coherence time, τ_0, and the refractive index structure parameter, C_N^2. Of these three, it is C_N^2 that is the basis on which the other two are built.

The coherence length is roughly the transversal distance over which the phase fluctuations is 2π. The coherence time is the same as coherence length but with respect to time, thus the coherence time is roughly the time for which the phase fluctuations in a point is 2π. The refractive index structure parameter is dependent on the altitude and the wind velocities there. With some calculations, taking the wind velocities at many altitudes gives a wind profile, that is the C_N^2 where $N = n - 1$ and n is the refractive index of the medium.

The C_N^2 is quite hard to get in practice due to the instruments needed to get data about the wind at different altitudes. At the institute, equipment of this kind is not available, this means that in order to get r_0 and τ_0 some approximations on C_N^2 are needed.

For this project there are several steps. First doing theoretical calculations to see if the setup, see section 7, that is planned to be used can be used for the intended purposes. The purpose is to to get r_0 values for the horizontal plane at different distances starting at short distances. If the setup can be used for the intended purposes, observations will be done. Based on the results from the observations new calculations will be done to see if further work at longer observational distances can be done and predictions on the possible results will be made. If it is possible to do longer distance observation these will be carried out. The results of these observations will then be checked against the predictions. Doing this for day and night time observations will give a good theoretical basis for further work in the field.

If the setup at any stage is not suited for observations according to the theoretical calculations, then the plan is to see what needs to be changed in order to make observations possible.

3 Theory

This section will deal with the mathematical theory behind the different parameters mentioned in the previous section. Some more in depth explanations about the various parameters, C_N^2, r_0 and τ_0 can also be found here. Lastly, the section also takes up mathematical equations used for the flux calculations done in this thesis work. The reason for the flux calculations are also discussed.

3.1 Refractive index structure parameter, C_N^2

C_N^2 is a non-stationary random function and can be expressed using structure functions which gives the variance of the difference in two locations. From Knutsson [8] and Tatarski [13] the equation for C_N^2 is:

$$C_N^2 = \frac{\langle |n(\mathbf{r}) - n(\mathbf{r} + \boldsymbol{\rho})|^2 \rangle}{\rho^{2/3}} \tag{1}$$

Here n is the refractive index of the air and $\boldsymbol{\rho}$ and $\mathbf{r}$ are 3d position vectors and ρ is the norm. Models of the C_N^2 profile has been done by for example Hufnagel and Valley, see Valley [14]. The model profiles shows that turbulence is strongest closest to the ground:
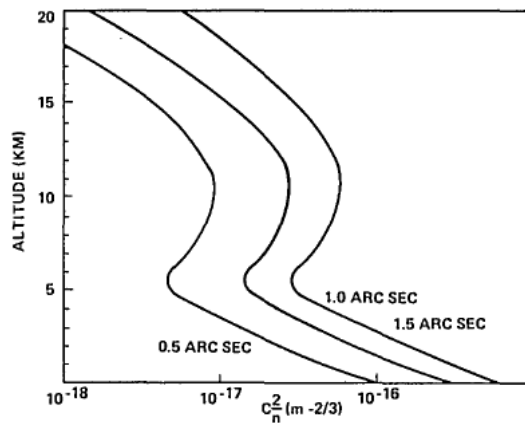

Figure 1: Hufnagel 1974, C_n^2 model scaled for seeing of 0.5, 1.0 and 1.5 arcsec at $\lambda = 0.55\mu m$

Even though the profile changes fast in the ground layer it can be assumed for this thesis that it is constant since the vertical thickness of the layer that will be studied is very thin in relation to the profile change.

3.2 Coherence length, r_0

As mentioned above, the coherence length is roughly the transversal distance over which the phase fluctuations is 2π. This can be understood from the following image together with the following mathematical derivation:
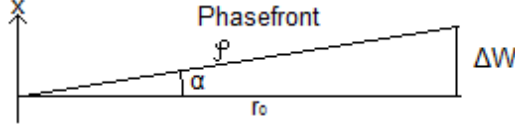

Figure 2: An incoming phase front, where α is the angle of excursion, φ is the phase front width and r_0 is the coherence length. ΔW is the distance from the phase front to the direction that is perpendicular to the phase front propagation direction. The light wave is traveling in the x-direction.

Using that the phase change, φ, is equal to $\frac{2\pi}{\lambda}\Delta W$ and that it fluctuates, it is possible to understand from the image that:

$$\sigma_\varphi^2 = \left(\frac{2\pi}{\lambda}\right)^2 \sigma_{\Delta W}^2 = \left(\frac{2\pi}{\lambda}\right)^2 r_0^2 \sigma_\alpha^2 = (2\pi)^2 \tag{2}$$

Here σ_φ^2 is the variance in the phase fluctuations and σ_α^2 is the variance in the angle of excursion. $\sigma_{\Delta W}^2$ is the variance in distance from the phase front to the direction that is perpendicular x direction.

From equation 2 it can be seen that:

$$\sigma_\alpha^2 = \left(\frac{\lambda}{r_0}\right)^2 \tag{3}$$

This shows the relation between the coherence length and the variance in the angle of excursion.

A more precise way to state what the coherence length is that up to a diameter equal to the coherence length the resolution of a telescope is dependent on the diameter, D, of the telescope, above which the resolution remains constant. This is due to the phase fluctuations and this can be expressed in the following equation, see Hardy [7]:

$$\sigma_\varphi^2 \sim \left(\frac{D}{r_0}\right)^{5/3} = 1, \text{ for } D = r_0 \tag{4}$$

As was stated before r_0 is dependent on C_N^2 as can be seen in the following equation, Knutsson [8] and Fried [4]:

$$r_0 = \left(0.432 k^2 [cos(\gamma)]^{-1} \int C_N^2(h) dh\right)^{-3/5} \tag{5}$$

Here $[cos(\gamma)]^{-1}$ is the air mass that the wavefront passes through, γ is the zenith angle of the telescope at and h is the altitude. k is the wave-number and is $\frac{2\pi}{\lambda}$ where λ is the wavelength of the light.

As was stated earlier, it can be assumed for this thesis that the C_N^2 can be set constant over the propagation path. Using this it becomes simple to predict coherence length at other distances, r_{0x}, when the coherence length is known for one distance, r_{0y}:

$$r_{0x} = r_{0y} \frac{\left(0.432 k^2 (cos(\gamma))^{-1} C_N^2 \int_0^x dh\right)^{-3/5}}{\left(0.432 k^2 (cos(\gamma))^{-1} C_N^2 \int_0^y dh\right)^{-3/5}} = r_{0y} \left(\frac{cos(\gamma)^{-1} \int_0^x dh}{cos(\gamma)^{-1} \int_0^y dh}\right)^{-3/5} \quad (6)$$

For this thesis the zenith angle does not change and thus the previous equation turns into:

$$r_{0x} = r_{0y} \left(\frac{x}{y}\right)^{-3/5} \quad (7)$$

Keeping in mind that this is only valid when the weather is more or less the same. This gives an opportunity to do predictions. By doing observations at one distance and calculating the coherence length it is possible to predict what the coherence length will be for any other distance, assuming that C_N^2 is constant.

To get the coherence length the average image displacement is put into the following equation, see Greenwood & Fried [6] (adapted for this project):

$$r_0 = \left(\frac{0.364 \cdot \lambda^2}{<\alpha^2> \cdot D^{1/3}}\right)^{3/5} \quad (8)$$

Here λ is the wavelength and it is dependent on what is targeted, D is the diameter of the telescope, here 0.364 m. $<\alpha^2> = <\alpha_x^2> + <\alpha_y^2>$ is the mean value of the squared angular displacement. This will be explained in deeper detail a bit further down. Equation 8 is valid for image exposure times shorter than the coherence time.

Here is a good place to note that the average angular image displacement needs to be in radians in equation 8, thus a conversion factor that converts from unit pixel (the cameras natural image unit) to unit radians is needed. The camera that is used to collect the data in this thesis is a QImaging Rolera-XR CCD camera , see QImaging [11]. For the setup used during this thesis, see section 7, each pixel has the field of view of 0".106 by 0".106. The pixel field of view is given by the following equation:

$$\alpha_{pix} = \frac{\Delta_{pixSC}}{S'} \frac{180 \times 3600}{\pi} \ [arcsec] \quad (9)$$

5

In this equation Δ_{pixSC} and S' are the pixel size for the science camera (SC) and the distance from the image space principal plane to the image plane. Any optical image capturing system can in essence be reduced to a single lens and imaging plane, as visualized in the following image:
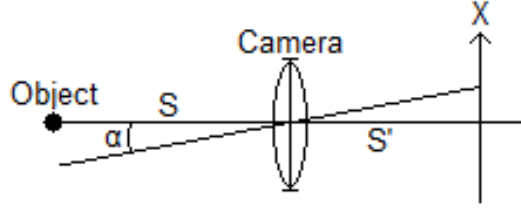

Figure 3: The simplest version of an imaging system. α is the angle of excursion, S is the distance to the imaging object and S' is the distance from the imaging system lens to the imaging plane. Note that $\sigma_x^2 = S'^2 \times \sigma_\alpha^2$

In the case of this thesis the "camera" in figure 9 represents the entire AO-setup,which will be described in detail in section 4. As long as the focus length for the SC, f_{SC}, is much shorter than the distance from the telescope primary lens to the imaging object, which it is in this thesis, the following approximation can be used:

$$S' = \frac{S f_{SC}}{S + f_{SC}} \sim f_{SC} \qquad (10)$$

Thus f_{SC} can be used instead of S' in equation 9.

For the Rolera-XR each pixels has sides of $13.7 \mu m$ and the focus length is 17.1 meters. The SC focal length of the imaging system is calculated section 7 with equation 40.

The FoV for the entire CCD array for the WFS can be calculated using the following equation, see Knutsson [8]:

$$\alpha_{FoV} = \frac{N_{LL} D_{LL}^2}{D_{tel} f_{LL}} \frac{180 \times 3600}{\pi} \ [arcsec] \qquad (11)$$

In this equation N_{LL}, D_{LL} and f_{LL} are the number, diameter and focus length of the lenslets of the WFS. D_{tel} is diameter of the clear aperture of the celestron telescope. For the setup used during this thesis work, see section 7, the values are 5, 336×10^{-6} m, 21.5×10^{-3} m and 0.356 m respectively, see Knutsson [8]. This gives a FoV of 14".8 by 14".8. This is the value that is used when mentioning the FoV in the rest of the thesis, unless otherwise specified.

The theory behind how the image displacement from one frame to another frame is tracked is described in section 3.4 and the program used is explained

in section 5.2. The result is naturally acquired in unit pixel as previously stated. These pixel values are thus multiplied by 0.106 (the FoV divided by the illuminated width measured in pixels on the SC) and divided by $\frac{180 \cdot 3600}{\pi} \approx 206265$ to convert it into radians. $< \alpha^2 >$ is thus the mean value of the squared displacement in radians when multiplied with $0.106 \cdot \frac{180*3600}{\pi}$.

3.3 Coherence time, τ_0

As stated before the coherence time is roughly the time for which the phase fluctuations in a point stays below 2π. Just as with coherence length there are other ways to state what the coherence time is: The coherence time is the time-scale over which the changes in the turbulence become significant. It is also the maximum integration time that can be used without losing information about the coherence length due to smearing of the image when using equation 8.

The expression for the coherence time is, Fried [5]:

$$\tau_0 = \left(2.91k^2(cos(\gamma))^{-1}\int C_N^2(h)(V_{wind}(h))^{5/3}dh\right)^{-3/5} \quad (12)$$

Just as with the coherence length, $cos(\gamma)^{-1}$ is the air mass that the wavefront passes through, γ is the zenith angle of the telescope at and h is the altitude. $V_{wind}(h)$ is the wind speed at altitude h. k is the wave-number and is $\frac{2\pi}{\lambda}$ where λ is the wavelength of the light.

The coherence time can be calculated using the coherence length:

$$\tau_0 = 0.31\frac{r_0}{V_0} \quad (13)$$

Here V_0 is the vertical velocity component perpendicular to the light propagation direction, see Masciadri et al. [10]:

$$V_0 = \left(\frac{\int_0^\infty C_N^2(h)|V_{wind}(h)|^{5/3}dh}{\int_0^\infty C_N^2(h)dh}\right)^{3/5} \quad (14)$$

C_N^2 is the turbulence profile.

This thesis it is the horizontal velocity component perpendicular to the light propagation direction that is needed. As a substitute the average wind speed can be used as a rough estimate of V_0 taking into account the wind direction. This can be acquired from local weather broadcasts or estimating the wind speed and direction by looking at flags and similar objects. Thus replacing equation 13 with:

$$\tau_0 \approx 0.3\frac{r_0}{sin(\theta)V_l} \quad (15)$$

Here θ is the angle for the incoming wind with respect to the propagation direction of the light. V_l is the local average wind velocity. It is clear that this equation will go to infinity when the wind direction goes towards being aligned with the observation direction. The wind direction is estimated in steps of 45 degrees, e.g. north west or north. For this reason the smallest angle is set to 22.5 degrees away from being aligned with the propagation direction. This is reasonable to assume, since it is the maximum effect of the wind that is of interest and the wind direction fluctuates during observations.

The limit for the setup to handle the turbulence of the atmosphere was stated to be in the region of $r_0 = 0.05$ m. Using this and assuming a normal wind speed in Lund of 4 m/s it is possible to get an understanding of the longest integration time that should be used when gathering data using equation 15. It is assumed that the wind is perpendicular to the light propagation, $\theta = 90 => \ sin(\theta) = 1$. This gives an integration time of 0.004 s. The system was not used if the wind was higher than 8 m/s in which case the integration time should be 0.002 s. Assuming that the coherence length is short, e.g. 0.01 m and the wind is high e.g. 8 m/s the integration time should be 0.001 s. This would be the absolute worst case scenario.

Plot 1 in Appendix A shows the integration times for different coherence lengths with increasing transversal wind speeds. There are two lines that are parallel to the x-axis, the top line marks the 3 ms exposure time and the bottom line marks the 1 ms exposure time. It is interesting to note that the 0.05 m line crosses the 3 ms line at a wind speed of 5 m/s and that it does not cross the 1 ms below a wind speed of 8 m/s.

Several things needs to be taken in to account when choosing an integration time during observations. The first thing is equation 15 and that wind coming from an angle to the perpendicular direction decreases the perpendicular component. The second thing is the stated limit at 0.05 m where the setup should be able to handle image distortions. Also taking account for how well the human eye can interpret the image that is being captured, setting the exposure times between 1 and 3 ms during observations to get good coherence length data was reasonable. The latter criteria is purely observational and based on first hand experience, sometimes it was hard even at 3 ms exposure with gain set to 45 (explained in section 4.2.3) to see an image with any structure. Having integration times on this scale means that equation 8 is valid. The coherence time estimate is based on Taylors frozen layer model, in practice the atmosphere is also "boiling" which may reduce the max integration time, see Hardy [7].

3.4 Image movement and atmospheric profiles

The light coming from the object passes through moving pockets of differently refracting air, thus changing the angle of arrival of the light onto the telescope. If the light is then directed to some data capture device such as a video camera, the effect is that the image of a point source moves around.

The average movement is needed to get information about how the air behaves as a whole. At least for this thesis it is of little or no interest to know how the air moves every second but rather how it moves on average during one or parts of one data gathering session. For a single frame the displacement in an image can be expressed by:

$$< \alpha^2 > = < \alpha_x^2 + \alpha_y^2 > = < \alpha_x^2 > + < \alpha_y^2 > \tag{16}$$

Here $< \alpha_x^2 > = < \alpha_y^2 >$ are the displacements of the captured image between frames in the horizontal and vertical direction respectively.

By tracking the light image and storing information about how it moves in comparison to a specific point, the average movement can be calculated using one frame as a reference frame. For the difference between frames 1 and 2, where $\overline{\alpha}_1 = (\alpha_{1x}, \alpha_{1y})$ for frame 1 and $\overline{\alpha}_2 = (\alpha_{2x}, \alpha_{2y})$ for frame 2, the following is true:

$$< |\overline{\alpha}_1 - \overline{\alpha}_2|^2 > = < |\overline{\alpha}_2|^2 > + < |\overline{\alpha}_1|^2 > -2 < \overline{\alpha}_1 \cdot \overline{\alpha}_2 > \tag{17}$$

Since $< \overline{\alpha}_1 \cdot \overline{\alpha}_2 > = 0$ and $< \overline{\alpha}_1 >$ and $< \overline{\alpha}_2 >$ are uncorrelated, this gives that:

$$< |\overline{\alpha}_1 - \overline{\alpha}_2|^2 > = < |\overline{\alpha}_2|^2 > + < |\overline{\alpha}_1|^2 > \tag{18}$$

Because $< |\overline{\alpha}_1|^2 > = < |\overline{\alpha}_2|^2 > = < \alpha_{1x}^2 > + < \alpha_{1y}^2 > = < \alpha_{2x}^2 > + < \alpha_{2y}^2 >$, the following is true:

$$< |\overline{\alpha}_1 - \overline{\alpha}_2|^2 > = 2 < \alpha_1^2 > = 2 < \alpha_2^2 > \tag{19}$$

In the right hand part of equation 19 there is a "2" that alters equation 8 so that it can be utilized when having one frame as a reference frame:

$$r_0 = \left(\frac{2 \cdot 0.364 \cdot \lambda^2}{< |\overline{\alpha}_1 - \overline{\alpha}_2|^2 > \cdot D^{1/3}} \right)^{3/5} \tag{20}$$

3.5   Variance estimation

In this thesis the image motion is used to get the coherence length, in extension also the coherence time. This is done by analyzing data images using Fourier transform analysis. Any information about aberrations or error effects, be it from the setup or the atmosphere are fused in the image content (excluding any computational error or computational approximation that might occur). As such the variance in the data set can be calculated using the same image data that was used to get the coherence length.

The image motion is random around some central point, this is described by a standard distribution function:

$$p(\alpha) = \frac{1}{\sigma^2}\alpha e^{-\frac{\alpha^2}{2\sigma^2}}, \; \alpha = \sqrt{\alpha_x^2 + \alpha_y^2} \tag{21}$$

Here α is the displacement of an image in two dimensions in comparison to another image and σ is the variance of α_x or α_y.

To get the standard deviation of the variance in the image motion the following equation can be used:

$$\sigma_{\alpha^2}^2 =< \alpha^4 > - < \alpha^2 >^2 \tag{22}$$

Using equation 21 to express $< \alpha^2 >$ and $< \alpha^4 >$ the following is acquired using standard extensions and variable substitution:

$$
\begin{aligned}
< \alpha^2 > \;&=\; \frac{1}{\sigma^2}\int_0^{\inf} \alpha^3 e^{-\frac{\alpha^2}{2\sigma^2}} d\alpha \\
&=\; \frac{1}{\sigma^2}\frac{1}{2}(2\sigma^2)^2 \int_0^{\inf} x e^{-x} dx \\
&=\; 2\sigma^2\left[-xe^{-x} \,|_0^{\inf} + \int_0^{\inf} e^{-x} dx \right] \\
&=\; 2\sigma^2,
\end{aligned}
\tag{23}
$$

where $\sigma^2 =< \alpha_x^2 >=< \alpha_y^2 >$. Hence $< \alpha^2 >= 2\sigma^2 =< \alpha_x^2 > + < \alpha_y^2 >$. In this and the next equation the variable substitution that is used is $x = \frac{\alpha^2}{2\sigma^2}$ and thus $dx = \frac{\alpha}{\sigma^2}d\alpha$.

$$
\begin{aligned}
< \alpha^4 > \;&=\; \frac{1}{\sigma^2}\frac{1}{2}(2\sigma^2)^3 \int_0^{\inf} x^2 e^{-x} dx \\
&=\; (2\sigma^2)^2\left[-x^2 e^{-x} \,|_0^{\inf} + \int_0^{\inf} 2x e^{-x} dx \right] \\
&=\; 2(2\sigma^2)^2
\end{aligned}
\tag{24}
$$

10

Now that $< \alpha^2 >$ and $< \alpha^4 >$ is available, they can be combined with equation 22 to give:

$$\sigma^2_{\alpha^2} = (2\sigma^2)^2 - 2(\sigma^2) = 2\sigma^2. \tag{25}$$

Taking the average of this expression for the n images gives:

$$\sigma^2_{<\alpha^2>_n} = \frac{1}{n}\sigma^2_{\alpha^2} = \frac{2\sigma^2}{n} \tag{26}$$

By dividing the mean variance for n measurements with the mean deviation it is clearly seen that the mean variance is one n:th of the mean deviations:

$$\frac{\sigma^2_{<\alpha^2>_n}}{< \alpha^2 >_n} = \frac{1}{n} \tag{27}$$

The equation can be used to check the results of the analyzed data to see if it is good. If the result differs from the $\frac{1}{n}$ then there is some error source in the measurements. If this difference is small, then the method to get coherence length is robust. As stated before there is one image that is used as a reference to all the other $n-1$ images, this means that for n measurements of α^2 gives $n-1$ measurements of α^2_{xy}. This means that:

$$\frac{\sigma^2_{<\alpha^2>_{xy}}}{\left(< \alpha^2 >_{xy}\right)^2} = \frac{1}{n-1} \tag{28}$$

From equation 8 the following is true:

$$\frac{\sigma^2(< \alpha^2 >)}{< \alpha^2 >} = \left(\frac{3}{5}\right)^2 \frac{1}{n-1} => \tag{29}$$

$$\frac{\sigma_{r_0}}{r_0} = \frac{3}{5}\frac{1}{\sqrt{n-1}}$$

If $< \alpha^2 >$ is based on measurements of n values of α and σ^2 is the variance in the image movement.

Thus, by multiplying the coherence length values with $\frac{3}{5}\frac{1}{\sqrt{n-1}}$ the variance of the coherence lengths are acquired.

3.6   Flux calculations

To fully understand the following equations, a basic idea of the equipment used during this thesis can be of use. The following figure shows the parts that are essential to the flux equations.
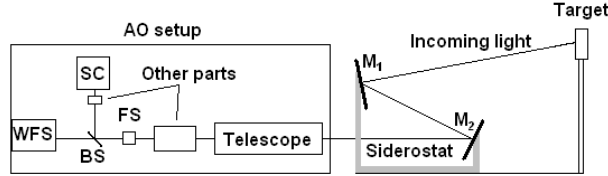

Figure 4: This figure only shows the equipment parts that are essential to the flux equations.

In figure 4, WFS and SC are the wave front sensor (WFS) and the SC. BS and is a pellicle beam-splitter and FS is a field stop. M_1 and M_2 are the primary and secondary mirrors of the siderostat respectively. An in depth discussion about the parts can be found in section 4. Some information about the parts is however integrated into the coming text.

There was a need to do flux calculations during the thesis to see if the WFS and the SC could handle the amount of light hitting them before doing any experiments. The results of the calculations can be seen in section 6.1.

The number of photons hitting one pixel in the WFS on average can be calculated with the following equation:

$$n_x = \int_0^{\tau_{int}} \int_{\lambda_1}^{\lambda_2} \frac{\lambda}{hc} D_{LL}^2 \frac{D_{tel}^2}{D_{SH}^2} \frac{\omega_{pix}}{\omega_x} T_{opt}(\lambda) F_x(\lambda, M) R(\lambda) d\lambda dt \qquad (30)$$

The equation is basically acquired from Knutsson [8]. The equation has however been modified. $R(\lambda)$ is the spectral response for each of the detectors, see e2v technologies [1] for the WFS and QImaging [11] for the SC. In Knutsson [8] the wavelength region used is 700-800 nm (set by a filter that has been removed for this thesis) and the spectral response is set constant within this region. In this thesis the wavelength region is between 200-1100 nm and the spectral response is dependent on the wavelength.

In this equation the n_x stands for the number of photons hitting each pixel in the detectors coming from some target. In this thesis the photons are from either the Moon, the LED target light or the photons that are reflected of a resolution target illuminated by the Sun and reaching the detectors. These targets are explained more in depth in section 4. The three light paths will from here on be referred to as moon, LED and STM (Sun Target

Mirror) respectively. The mirror in "STM" refers to the primary mirror of the telescope.

λ is the wavelength, h is the Planck's constant and c is the speed of light. D_{LL} is the physical lenslet diameter in the Shack Hartmann WFS, D_{tel} is the diameter of the telescope primary mirror and D_{SH} is the diameter of the pupil image on the lenslets. $\frac{D_{LL}}{D_{SH}} = \frac{1}{5}$ and ω_{pix} is the solid angle of the pixels and is calculated by taking the FoV divided by the number of pixels in the subimage or the area that sees the light and finally square the answer because it is a square surface. The number of pixels in each subimage is $\frac{80}{5} \cong 16$. ω_x is the solid angle of the light reflectors/emitter (the Moon, the resolution target or the LED). T_{opt} is the optical transmittance (which is different for the two cameras due to the beam splitter that divides the light 90%/10% to the WFS and SC respectively) of the system and F_x is the incoming intensity from the targets.

The same equation can be used for the SC with some slight changes. $\omega_{pix,WFS} = \left(\frac{14.8}{16}\right)^2$ and $T_{opt,WFS} = 0.9$ for the WFS and $\omega_{pix,SC} = \left(\frac{14.8}{140}\right)^2$ ($\sim$ 140 by 140 pixels in FoV, calculated in section 4.2.3) and $T_{opt,SC} = 0.1$ for the SC. There is also a direct change in equation 30 going from the WFS to the SC, the difference is that D_{SH}^2 and D_{LL}^2 are removed since the number of photons are collected over the full aperture D_{tel}.

The atmospheric transmittance, T_{atm}, is incorporated into the flux, $F_x(\lambda, M)$, which is the following:

$$F_x(\lambda, M) = F_x(\lambda)T_{atm}(\lambda, M) \tag{31}$$

Studying the equations and thinking logically there are only in principal three things that differ the number of photons incoming for the moon in comparison with the amount of photons coming from the light reflected of the target. The differences are the angular size of the light reflectors, ω_x, the irradiance, F_x, from these and the distance to the targets.

As already mentioned there are for this thesis three types of targets, the Moon, an LED and the resolution target. Thus three expressions are needed for F_x, one for each target type. The lunar irradiance can be acquired from Knutsson [8], equation 3.2 page 38:

$$F_{moon} = \frac{P(\lambda)\Phi(\beta)}{\pi d_{moon}^2} F_\odot(\lambda)\pi r_{moon}^2 = \frac{P(\lambda)\Phi(\beta)F_\odot(\lambda)r_{moon}^2}{d_{moon}^2} \tag{32}$$

Here P is the lunar albedo, Φ is the lunar phase angle function, r_{moon} and d_{moon} is the radius and distance of and to the moon respectively. $F_\odot$ is the solar irradiance.

The irradiance from the Sun via the resolution target getting to the siderostat is:

$$F_{STM}(\lambda) = F_\odot(\lambda)cos(\theta_1)cos(\theta_2)\frac{kA_T}{\pi r_{TM}^2} \tag{33}$$

Here k is the reflective coefficient of the target, A_T is the area corresponding to the FoV of that target and r_{TM} is the distance from the target to the entrance aperture of the telescope. $F_\odot$ is the irradiance of the Sun. The cosine angles are for the angles from the normal of the target to the Sun, θ_1, and from the normal of the target to the siderostat primary mirror, θ_2.

Plots 2 and 3 in Appendix A shows the solar flux and the lunar albedo. Their x-axis shows the wavelength. The y-axis shows the intensity for the solar flux plot and the albedo for the lunar albedo plot.

Equation 33 can with two minor changes be applied to the LED target. Changing the solar irradiance to that of the LED, F_{LED}, and removing $cos(\theta_1)$ since it is the target it self that is emitting the light and not reflecting the solar light. Note here that if the resolution target or the LED target is tilted so that they are placed face on (parallel) with respect to the siderostat primary mirror then $\theta_2 = 0$ and $cos(\theta_2) = 1$. This will always be the case in this thesis. Note that this face on angle for the resolution target implies that the angle from the target normal to the Sun increases the same amount that that would otherwise be between the target normal and the siderostat primary mirror.

Because the resolution target should fill the FoV of the WFS for the best possible result, the area of the resolution target, A_T, is calculated with the following equation:

$$A_T = r_{TM}^2 \times \alpha_{FOV}^2 \tag{34}$$

Here α_{FOV} is field of view of the WFS and is 14".8 by 14".8. Because there is a field stop that this adjusted to the WFS FoV, the SC will never see more than 14".8 by 14".8. The area of the Moon and the LED are not set by the author.

Now that all the parts of equation 30 has been addressed, it would be a good idea to take a look at it again to see if it can be simplified. With this in mind, many of the factors can be taken out of the integrals since they are not dependent on the integration time or the wavelength, the equation thus becomes (for the Moon, the LED and the resolution target respectively):

$$n_{moon} = \frac{D_{LL}^2}{hc}\frac{D_{tel}^2}{D_{SH}^2}\frac{\omega_{pix}\Phi(\beta)r_{moon}^2}{\omega_{moon}d_{moon}^2}...$$

$$\int_0^{\tau_{int}}\int_{\lambda_1}^{\lambda_2}\lambda T_{opt}(\lambda)T_{atm}(\lambda)P(\lambda)F_\odot(\lambda)R(\lambda)d\lambda dt \tag{35}$$

This is for the Moon, the next version is for the LED:

$$n_{LED} = \frac{D_{LL}^2}{hc} \frac{D_{tel}^2}{D_{SH}^2} \frac{\omega_{pix}}{\omega_T} \frac{kA_T}{\pi r_{TM}^2}...$$

$$\int_0^{\tau_{int}} \int_{\lambda_1}^{\lambda_2} \lambda T_{opt}(\lambda)T_{atm}(\lambda)F_{LED}(\lambda)R(\lambda)d\lambda dt \qquad (36)$$

and finally for the resolution target:

$$n_{STM} = \frac{D_{LL}^2}{hc} \frac{D_{tel}^2}{D_{SH}^2} \frac{\omega_{pix}}{\omega_T} \frac{kcos(\theta_1)A_T}{\pi r_{TM}^2}...$$

$$\int_0^{\tau_{int}} \int_{\lambda_1}^{\lambda_2} \lambda T_{opt}(\lambda)T_{atm}(\lambda)F_{\odot}(\lambda)R(\lambda)d\lambda dt \qquad (37)$$

Note that in equation 35 $\frac{r_{moon}^2}{\omega_{moon}d_{moon}^2} = 1$. Furthermore, note that it is only equation 37 that is dependent on the angle from the target normal to the Sun. The same changes to these equations can be done to go from the WFS to the SC as stated before.

The distance to the Moon be can considered constant and since it is the maximum flux that is of interest, the phase angle of the Moon is also constant (=1, corresponding to full Moon). The reflective coefficient for the paper that the resolution target is printed on be set to 1 (meaning that all light is reflected). The optical transmittance for the setup can be seen as approximately constant. With these approximations five variable remain inside the integrations, λ, $R(\lambda)$, $F_{\odot}(\lambda)$, $F_{LED}(\lambda)$ and T_{atm}. The equation results in the number of photons that on average hits a pixel per integration time either from the Moon, the LED or from the Sun reflected of the resolution target and reaching the setup.

Table 2 shows the parameters used for the case of the closest target (70 m). The reason for this using distance and why it was calculated will be discussed in section 5.1.3. The distance only effects the LED since that is the only target that does not scale with distance. The Moon has a constant distance. In the case of the resolution target the light will always be the same no matter the distance since its area is scaled according to distance.

The values are sorted according to if they are constants or if they are variables. The integration regions are set separately. The results of the flux calculations are shown in the result section, section 6. The distance to and the diameter of the Moon together with its angular size is included even though they become 1 in equation 35. In table 2 Res stands for the LED and resolution targets.

Table 2: List of equation parameters for the WFS

Constants	Variables
$c = 3 \times 10^8$ [m/s]	λ [m]
$h = 6.626 \times 10^{-34}$ [Js]	$F_\odot(\lambda)$ [W/m^2]
$k = 1$ [-]	$F_{LED}(\lambda)$ [W/m^2]
$\Phi(\beta) = 1$ [-]	$P(\lambda) = 0.0002 \times \lambda$ [-]
$T_{opt,WFS}(\lambda) = 0.9$ [-]	$T_{atm}(\lambda)$ [-]
$T_{opt,SC}(\lambda) = 0.1$ [-]	$\theta_1 = 0$ [degree]
$D_{tel} = 0.365$ [m]	$\theta_2 = 0\text{-}80.9$ [degrees]
$D_{LL} = 325 \times 10^{-6}$ [m]	**Integration regions**
$D_{SH} = 0.0123$ [m]	$\lambda_{1,Res} = 200 \times 10^{-9}$ [m]
$A_{CCD,WFS} = 3.69 \times 10^{-6}$ [m^2]	$\lambda_{2,Res} = 1100 \times 10^{-9}$ [m]
$A_{CCD,SC} = 2.71 \times 10^{-6}$ [m^2]	$\lambda_{1,LED} = 610 \times 10^{-9}$ [m]
$A_{T,Res} = 33.4 \times 10^{-6}$ [m^2]	$\lambda_{2,LED} = 660 \times 10^{-9}$ [m]
$A_{T,LED} = 11.37 \times 10^{-6}$ [m^2]	$\tau_{int} = 1 \times 10^{-3}$ [s]
$\omega_{pix,WFS} = (14.8/16)^2$ [$arcsec^2$]	**Lunar values**
$\omega_{pix,SC} = (14.8/140)^2$ [$arcsec^2$]	$\omega_{moon} = 0.2 \times 60^4$ [$arcsec^2$]
$\omega_{T,Res} = 14.8^2$ [$arcsec^2$]	$r_{moon} = 1737.4 \times 10^3$ [m]
$\omega_{T,LED} = 11.47^2$ [$arcsec^2$]	$d_{moon} = 384399 \times 10^3$ [m]
$r_{TM} = 68$ [m]	

4   Equipment

The equipment used during this thesis work was an AO-setup, a siderostat, a LED/resolution target, a 0.3 meter mirror and computers. Note that either the LED or the resolution target will be used depending on if it is used to get the coherence length or to test the capability of the setup with something that is not self luminous.

The LED/resolution target will be discussed and so will the use of the 0.3 meter mirror later on in this section.

The AO-setup is the same setup used in Knutsson [8]. The setup will thus just be discussed briefly and for more information, see Knutsson [8]. There were some modification done to the setup, these modifications will be addressed in somewhat greater detail.
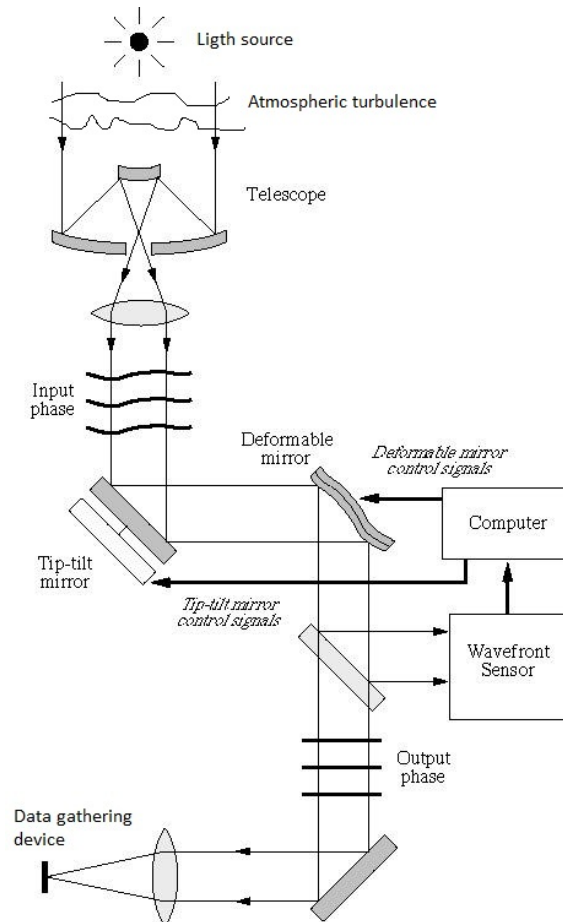

Figure 5: A schematic of an generic AO-setup.

4.1 A generic AO-setup

To begin with, the basics of an adaptive optics setup will be discussed. There are several components in an AO-setup that are always present in one form or another. The first part is some form of light gathering device, a telescope that directs the light, wavefront, into the system. The next two crucial components are one tip-tilt mirror and one or more deformable mirror(s) depending on weather the system is designed for single or multiple conjugate adaptive optics. A semi-transparent mirror or beam-splitter that directs some percentage of the light to a wavefront sensor to be used for sensing the wave front and the remaining percentage to be used for data gathering and experimenting. A sketch of a generic AO system can be seen in figure 5. Apart from these components there may be any number of refocusing lenses, mirrors and beam-splitters to redirect the light. The different parts of an AO-setup need to be explained in order to get an understanding of how the coherence length and coherence time effects the design of an AO-setup.

4.1.1 The Wavefront Sensor

When the wavefront passes through the atmosphere it gets distorted. The distorted wavefront is focused with the telescope on the AO-setup. In the AO-setup the wavefront is reflected by the tip-tilt mirror and the deformable mirror(s) and sent on to a beam-splitter or a semi transparent mirror. The wavefront is spread across the WFS's CCD detector plane via a lenslet array, see figure 6.
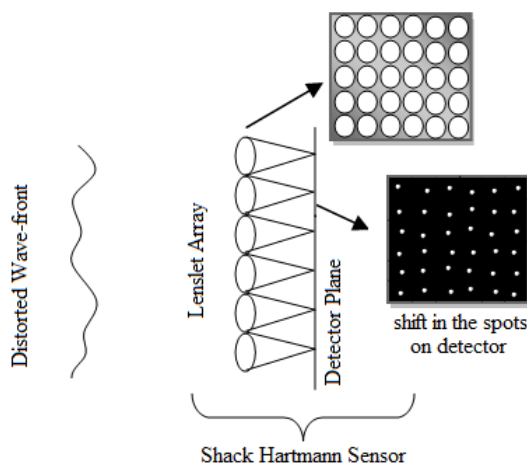

Figure 6: This shows a lenslet array of a Shack-Hartmann WFS with displacements of the focii caused by a distorted wavefront.

Each lenslet focuses it's part of the wavefront onto a subimage on the CCD. The lenslet array is placed at a plane conjugate to the entrance pupil, and thus the WFS can sample the wavefront at the subapertures. How much the WFS can see, the field of view (FoV), is determined by the number of lenslets covered by the pupil image, the lenslet focus length and the celestron telescope clear aperture diameter. This can be calculated using equation 11, found in section 3.2.

The number of photons hitting each pixel in the WFS for a set target intensity is determined by the integration time which must be shorter than the coherence time, τ_0, to avoid smearing off the instantaneous local tip/tilt measured at a subaperture. Since r_0 describes what is happening in the atmosphere with the wavefront, it follows that r_0 also determines how the wavefront is distributed over the subapertures. Thus it is r_0 and the size of the entrance pupil, D_{tel} that determines how many wave front samples and how many actuators there should be on the deformable mirror(s) to be able to handle the distortions of the atmosphere. The width of the subapertures projected back on the telescope entrance pupil should be equal to of smaller than r_0. The number of actuators, N_a, should be on the same order as:

$$\left(\frac{D_{tel}}{r_0}\right)^2 \tag{38}$$

This equation is acquired from Esposito [3]. The actuator pitch must be smaller than r_0, which it becomes if the actuators are equally spaced and the number of actuators equal to N_a.

If the incoming wavefront is a plane wavefront, each subaperture sees the same pattern. This pattern is shifted the same amount in each image with respect to the center point. If the wavefront is not plane (as it usually is not) each subaperture will see a different local tilt. A computer connected to the WFS does a correlation analysis of the entire subaperture plane with respect to some reference. The resulting matrix of the analysis is sent to the tip-tilt mirror and the deformable mirror(s). How many times this is needed each second is decided by the coherence time.

4.1.2 The tip-tilt mirror

The tip-tilt mirror is basically a mirror that can be angled around two perpendicular axes, both of which are perpendicular to the propagation direction of the light. It is the information about the part of the shift that is the same for all the subapertures caused by the wavefront that is sent to the tip-tilt mirror. The tip-tilt mirror thus tips and tilts to correct for this shift.

4.1.3   The deformable mirror

The deformable mirror(s) have actuators that poke the mirror(s) to deform them. It is the information about the part of the local wave front tilt that is not the same for all the subapertures that is sent to the deformable mirror(s). Each actuator is given a command to poke the mirror a certain amount so that the total sum of all the actuator pokes results in a reflected plane wavefront. The poke amount for each actuator is held constant until the next command arrives.
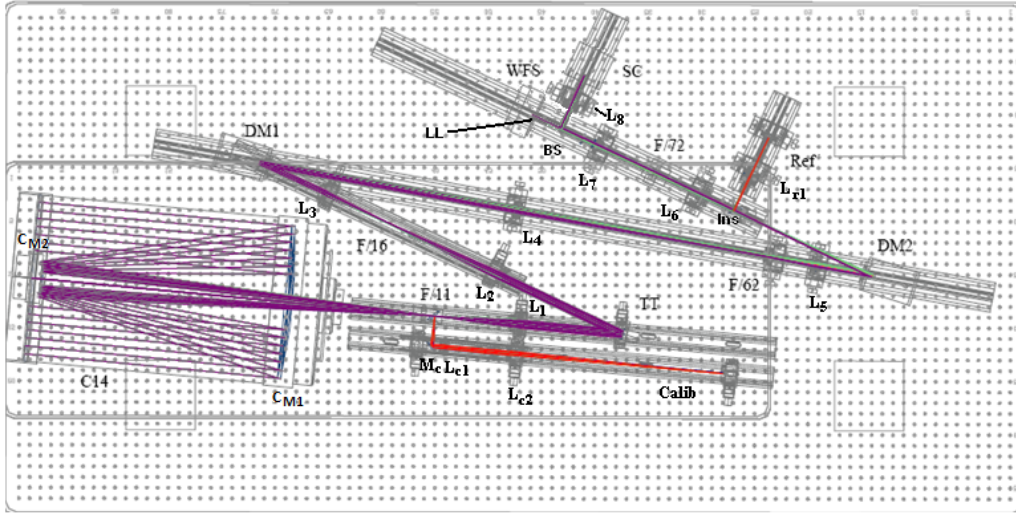

Figure 7: This shows the positions of the different components and the different focal ratios in the focii for the local setup.

4.2   The local setup

As mentioned the AO-setup is the same setup used in Knutsson [8] with some small changes. In this section the AO-setup will be explained in detail. An sketch of the AO-setup is useful for clarity: In figure 7 C14 is a Schmidt-Cassegrain celestron, TT is a tip-tilt mirror. C_{M1} and C_{M2} are the primary and secondary mirrors of the celestron respectively. DM1 and DM2 are the first and second deformable mirrors which have 35 actuators each that takes 5 ms to reach 80% of the peak value and are developed by OKO Tech. WFS is a Shack-Hartman wave front sensor and SC is a QImaging Rolera-XR CCD camera with which the experimental results used in this thesis are recorded.

LL is the lenslet array that is placed infront of the WFS. L_1-L_8, L_{c1}, L_{c2} and L_{r1} are all lenses. M_c is a mirror in the calibration arm. The F/x are the different focal ratios at all the focii. Finally Calib and Ref are the calibration and reference arms. All of these will be addressed and explained where they are placed and what they do in the order in which the light passes through or is reflected by them. The description will be divided into five parts; *Main structure*, *Calibration arm*, *Reference arm* and *Other parts*. The fifth and final part called *Changes to the setup* deal with the changes in comparison with the configuration used in Knutsson [8].

4.2.1   The siderostat

To get the light into the AO-setup a siderostat was used. The siderostat has two plane mirrors. The primary mirror has a clear aperture of 600 mm. This mirror can rotate perpendicular around the polar axis. The light that is reflected of the primary mirror is reflected via a stationary secondary mirror, with a clear aperture of 380 mm, into the room with the AO-setup. In this thesis the primary mirror is turned using a control computer where the commands are given directly to the motors by stating the wanted declination and hour angle. The maximum declination that can used is about ± 0.60 rad and the hour angle is about ± 2 rad.

Since the siderostat is placed outside and the AO-setup is inside there is a hole in the wall with a lid that can be opened and closed. When the AO-setup is in use, the light is sent to the primary mirror of the C14 celestron seen in figure 7.

4.2.2   Main structure of the AO-setup

Here it will be described how the light travels through the AO-setup and what happens along the way. After the description comes a table that has useful information on the different parts of the AO-setup.

The light comes in via the celestron reflecting of it's first and second mirror, C_{M1} and C_{M2}, and is focused at the focus point F/11. The celestron's diffraction limited angular resolution R_c can be calculated with the following equation:

$$R_c = 1.22 \frac{\lambda}{D_{tel}} \frac{180 \times 3600}{\pi} [arcsec] \tag{39}$$

The clear aperture, D_{tel}, of the celestron is 0.356 m. The wavelength of interest for this thesis is the standard wavelength set for the visible light (550 nm) and the peak wavelength of the red LED light that has been used,

see section 4.3 for more information. The red LED light peak wavelength is 635 nm, LEDZ [9]. These two wavelengths give resolutions of 0".32 for the 550 nm and 0".36 for the red LED. These values should roughly match the resolutions for the SC. These are calculated in section 4.2.3.

In the F/11 focus point a plane mirror can be inserted to block the incoming light from the celestron. Instead of the light from the celestron, light from the calibration arm can be directed into to the system. The calibration arm is described in section 4.2.4.

The light passes through lens L_1 so that the celestron pupil is imaged on the tip-tilt mirror. The tip-tilt mirror is used to correct for the vertical and horizontal displacement of the incoming light.

The light is reflected by the tip-tilt mirror and with the help of the an afocal combination lens pair L_2 and L_3 the celestron pupil is imaged onto the first deformable mirror, DM1. This deformable mirror does identical corrections for all points in the field.

The light is reflected by DM1 and passes through the L_4 lens which focuses the light on a field lens at the F/62 position. The field lens images an altitude of 10 km on DM2 after being collimated by L_5. DM2 corrects for anisoplanatism.

The reference arm can be inserted in between DM2 and L_6, this position is marked with "Ins" in figure 7.

A second afocal lens combination, L_6 and L_7, is used to magnify and image the celestron pupil on the WFS lenslet array. The field of view of the WFS is 14".8 by 14".8, calculated in section 4.2.3, and the WFS CCD array is comprised of 80 by 80 pixels with sides of 24 μm.

At the F/72 position in between L_6 and L_7, a field stop is placed. This field stop s used to match the incoming light to the field of view to the WFS lenslets or limit the field of view more if needed.

In between the L_7 and the WFS is a pellicle beam-splitter. This beam-splitter divides the light between the WFS and the SC at a ratio of 90%/10%. Lens L_8, an acromatic lens, is placed between the beam-splitter and the SC.

The effective focal length of the SC is calculated by using a basic optical equation, Knutsson [8]:

$$f_{SC} = \frac{f_8}{f_7} \frac{f_6}{f_5} \frac{f_4}{f_3} \frac{f_2}{f_1} f_{tel} \tag{40}$$

The focal lengths can be found in table 3. Using these focal lengths with equation 40 and the focal length of the celestron, 3910 mm, gives a focal length of 17106 mm for the complete imaging system. As mentioned before the SC pixels have sides that are 13.7 μm long.

Table 3: A list of the "components" shown in image 7. D_p is the distance from previous part in the setup. The column with "Other information" contains the focal lengths (fl) [m], diameters (d) [m], radius of curvature (rc) [m] or how the beam-splitter splits the light (split) [% to WFS/% to SC]. It is also stated where the calibration and reference arm are inserted.

Name	Object	D_p [m]	Other information
C14	celestron	—	—
C_{M1}	celestron mirror 1	6.160 from S2	0.362/1.5 (d/rc)
C_{M2}	celestron mirror 2	~ 0.9 from C_{M1}	0.089/0.447 (d/rc)
F/11	focus point	1.466 from C_{M2}	insert calib
L_1	lens	1.360 from C_{M2}	0.2 (fl)
TT	tip-tilt mirror	0.244 from L_1	0.025 (d)
L_2	lens	0.312 from TT	0.3 (fl)
L_3	lens	0.474 from L_2	0.16 (fl)
DM1	deformable mirror	0.255 from L_3	0.0097 (d)
L_4	lens	0.616 from DM1	0.6 (fl)
F/62	field lens	0.616 from L_4	-0.05 (fl)
L_5	lens	0.128 from F/62	0.12 (fl)
DM2	deformable mirror	0.128 from L_5	0.0097 (d)
Ins	—	0.358 from DM2	insert ref
L_6	lens	0.446 from DM2	0.14 (fl)
F/72	field stop	0.144 from L_6	—
L_7	lens	0.143 from F/72	0.15 (fl)
BS	pellicle beam-splitter	0.117 from L_7	90/10 (split)
WFS	WFS	0.260 from BS	17.106 (fl)
L_8	lens	0.053 from BS	0.10 (fl)
SC	lens	0.106 from L_8	17.106 (fl)

In table 3 all the components and insertion points are listed. The name of the components seen in figure 7, what the component is, the distance from the previous component D_p. In the column marked "other info" are information on focal length of the component, fl, the diameter of the mirrors, d, and the radii of curvature of the celestron mirrors, rc. $S2$ in the table is referring to the second mirror of the siderostat. $insert calib$ and $insert ref$ are where the calibration and reference arms are inserted into the main body of the setup.

4.2.3   The WFS and SC

There are two important cameras in this setup, the WFS and the SC. The WFS is used to get information on the wave front local tip/tilt. This information is then used to correct the wave front to make it as plane as possible. The SC is used to gather the data about the atmosphere. These data are used to get the coherence length and time.

It is important that the cameras fulfill certain criteria to get useful data that can later be analyzed. The most important aspects are the FoV and the pixel resolution. The FoV determines how big an object can be at a given distance to be contained within the image boundaries. The camera that captures the data, the SC, must have an equal or larger total FoV as the WFS to collect all the useful data. However, the area of the SC that is outside the area of the WFS will not contain any useful data since that area is not corrected for by the AO. Because of the field-stop both the WFS and the SC have the same FoV. Since the field is cut according to the area of a subimage in the WFS (i.e. 14 by 14 pixels in the WFS), any area that is outside of this in the SC will not get any photons that (not including image edge effects) and thus will not contain any useful information. It is thus the WFS FoV that is of interest. To get the FoV of the WFS equation 11 is used. For the setup used in this thesis the values are $N_{LL} = 5$, $D_{LL} = 336 \times 10^{-6}$, $f_{LL} = 21.5 \times 10^{-3}$ m and $D_{tel} = 0.356$ m. Inserting these into equation 11 gives the result 14".8 by 14".8 for the WFS FoV.

To give a deeper understanding of the WFS, the number of pixels on the CCD is 6400 (80 by 80) each pixel being 24 by 24 μm in size. Thus the entire CCD is 1920 by 1920 μm. The lenslet array divides the CCD into 25 subimages. Each subimage is thus comprised of 16 by 16 pixels with the total size being ~ 384 by 384 μm. This means that the pixel sampling is $\frac{14''.8}{16} = 0''.93$ for the WFS. This should be compared to the resolution calculated for 550 and 635 nm (visible light and the peak wavelength for the LED), which was 0".32 and 0".36 respectively. Because there are five subapertures across the field of the WFS these values should be multiplied by five. This gives 1".6 at 550 nm and 1".8 at 635 nm. This is close to the pixel sampling of the WFS, and it means that there is an under sampling in the WFS at these wavelengths.

Using this information and information about the distances from the beam-splitter to the WFS and the SC and the position of the L_8 lens, it is possible to calculate the number of pixels exposed on the SC. Looking in table 3, the distance from the beam-splitter to the WFS is 0.260 m, the beam-splitter to L_8 is 0.106 m and from L_8 to the SC the distance is 0.053 m. Thus the number of pixels covered in the SC FoV is: $\frac{0.260}{0.106} \frac{0.106}{0.053} \frac{384^2}{13.7} \approx 138^2$.

The only light that is seen by the WFS CCD is the light from the illuminated subapertures and the only light that the SC CCD sees is from the illuminated lenslets.

The resolution of the cameras is the other important criterion to be fulfilled for to get good data. To get the resolution, R, of a camera the following simple equation is used, the Nyquist equation:

$$R = 2\frac{\alpha_{FoV}}{n_{pix}} \tag{41}$$

In this equation α_{FoV} is just as in earlier equations the FoV of the camera. n_{pix} is the number of pixels across the FoV. The number two in the equation comes from the fact that two is the lest number of pixels needed to distinguish between two features. In the case of the WFS n_{pix} is the number of pixels in the subaperture, which is 16 for this setup giving a resolution of 2".41, this is about an order of magnitude lower resolution than that which was calculated for the telescope at 550 and 635 nm (for visible light and the LED). In the case of the SC, it is the number of pixels across the FoV that is of interest. This is about 140 pixels. This gives a resolution of 0".28 for the SC, which is the same order of magnitude as calculated for the telescope.

Now that the main part of the AO-setup has been described, the calibration arm and reference arm remains to be described.

4.2.4   Calibration arm

The light from the calibration arm is used to create an interaction matrix that tells the deformable mirrors how they are to respond to incoming light. Different types of apertures or patterns for the light can be used in the calibration arm to give different types of responses depending on the object that is to be observed. In this thesis three different patterns have been used; a pinhole, a grid of pinholes and a structure that is an image of the Moons surface. The Moon surface pattern was used during the initial phases of the thesis to get to know the system. The pinhole was used when observing "point sources" and the pinhole grid was used for the other observed objects, see section 4.3 for more information on this. The light from the pattern passes through an afocal lens pair that focuses the light at the F/11 point. These lenses are marked with L_{c1} and L_{c2} in figure 7, their focal lengths are 100 mm and 500 mm respectively.

As stated earlier, there is a flat mirror that can be lowered into the F/11 point. This is to cut of the light coming in from the celestron to use the light from the calibration arm instead. Due to space limitations in the setup location the calibration arm needs to be parallel with the structure in

between the celestron and the tip-tilt mirror, thus another plane mirror was used, marked M_c figure 7. The distance from the F/11 point to the mirror on the calibration arm is 69 mm and the distance from this mirror to the pinhole placement is 702 mm. The distances from the pinhole position to L_c1 and L_c2 is 675 mm and 496 mm respectively.

4.2.5   Reference arm

The reference arm is used to set the zero-points for the WFS. These zero-points are set to be a flat wavefront, the ideal to go for. The reference arm is also used as a reference for the calibration arm, to find where the center of the light path should be. In extension the reference arm is used to get rid of static aberrations in the setup. The image of the reference arm is focused at the F/72 point. From the reference arm light source to the WFS and SC there are no distortions.

    The light source in the reference arm is a point source formed by illuminating a pinhole. There are two lenses, L_r1 and L_r2 with focal lengths 140 mm and 100 mm respectively. As with the calibration arm there is a mirror that introduces the light into the main structure between DM2 and L_6 at a distance of 289 mm from DM2. The distance from the mirror to the pinhole is 193 mm.

4.2.6   Other parts

There is one more camera (the monitor camera) that is connected to the setup. The monitor is used as a visual aid to roughly direct the siderostat. This camera has a field of view of about a fourth or a sixth times the size of the Moon. The light is directed to the monitor camera via a mirror that can be moved in and out of the light path. That mirror is a plane mirror and is just after the celestron.

    One last thing about the setup should be mentioned here. In between DM2 and the insertion point of the reference arm a lens can be inserted to correct for possible astigmatism that is introduced by the deformable mirrors. This reduces the workload on the deformable mirrors This lens has no fixed position.

    All of the parts positions mentioned in the text above are the starting positions, these can all be changes to correct for any temporary effects such as temperature variations in the setup room. This is at maximum a few millimeters of displacement in the setup. For more detailed information about the setup, Knutsson [8].

4.2.7   Changes to the AO-setup

There are several changes to the setup in comparison to Knutsson [8], not all changes was made during this thesis. Some changes were made in the time after Par Knutsson ended his work and before this thesis began. The long-pass glass filter ($\lambda > 665nm$) was removed in order to pass light from the LED. The beam-splitter was changed so that now it is 90%/10% to WFS/SC. The positions of the WFS and the SC, including L_8 was interchanged. A filter holder, see figure 8, was constructed to be placed in the light path at the inner opening of the celestron. The inner opening of the celestron is where the light exits the celestron. The filter holder has a hole in it to let the light pass through. In this filter holder, one or more filters films can be added to reduce any light as needed during daytime observations. The filter used during this thesis were neutral density filter films with optical density values of 0.09. The filters are mostly used to be able to see anything in the monitor screen since the monitor camera gets saturated much earlier than the other two cameras, the WFS and SC, basically showing a white screen even when it is a cloudy day. The light is however needed when gathering data, thus the filter holder is removed before collecting data. The filter holder has been constructed for easy removal during observations. The filter holder specifications can be found in figure 8:
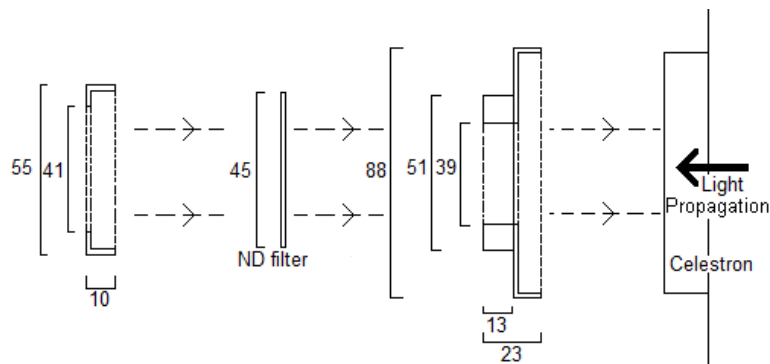

Figure 8: The filter holder for the neutral density filters. All parts are circular if seen with the light propagation as the central axis.

4.3   The targets

Here the different targets used during the thesis will be discussed. Also some information about a newly added small 0.3 m mirror will be described here.

4.3.1   The resolution target

For the AO to have something to work with a target was created on which a paper printout could be put. The paper printout images are used to test the resolution capabilities of optical sensors. The size of the resolution target is set to be equal to the full FoV of the setup, 14.8 $arcsec^2$ and can be seen in figure 9. The scale can be seen in the image. The red and green boxes and lines in the image is to explain the resolution of the cameras. Due to the fact that it was hard to focus on the resolution target a LED light was attached to the board with the resolution target, this LED was used for night time focusing.
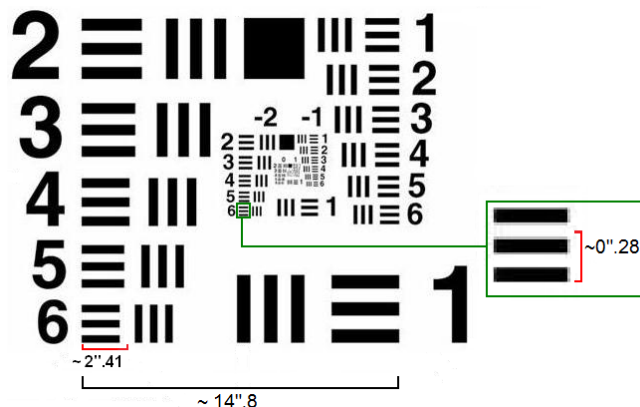
Figure 9: Resolution target image with guiding lines and scale size.

The resolutions calculated before for the WFS and the SC sets the limit for the smallest feature that can be discerned. The WFS's resolution size was 2".41, calculated in section 4.2.3, corresponds roughly to the size of the three lines that is next to number 6 that is on the bottom left side in the image, marked with a red box in the image. Note that these three lines would be roughly covered by 18 by 18 pixels in the SC.

The SC has a resolution of 0".28 calculated in section 4.2.3, corresponds to about the thickness of the two lines that is next to number 6 in the repeated inner image. In the image this region is enlarged in a green box and the thickness of one line is marked with a red line. Because of the atmosphere they should only be visible when the AO is working properly and should roughly be covered by 2 by 2 pixels in the SC.

4.3.2   New 0.30 meter mirror

During this thesis work a new 0.30 meter mirror was added to be able to see objects that is "behind" the siderostat and at long distances in the horizontal plane in the ground layer of the atmosphere. The primary mirror of the celestron is ~ 0.36 m. The distance from the primary mirror of the celestron to the 0.3 m mirror is ~ 25 m.

Unfortunately the diameter of the new 0.3 m mirror is smaller than the diameter of the celestron diameter. So to avoid vignetting there will be a maximum target distance. With the 0.3 m mirror the distance becomes 150 m using the following basic geometric equation:

$$d_T = d_{CM} \frac{D_T}{D_T - D_M} \tag{42}$$

Here D_M and D_T is the diameters of the 0.3 m mirror and the primary mirror of the celestron respectively. d_{CM} is the distance between the celestron primary mirror and the 0.3 m mirror and d_T is the distance to the target. This is illustrated in figure 10.
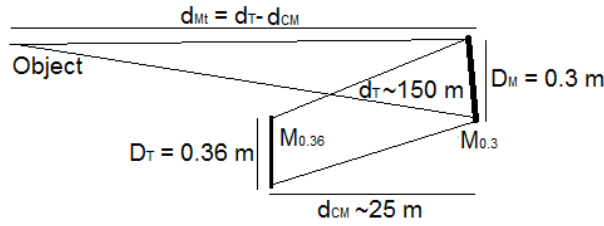
Figure 10: This illustration shows the minimal distance needed to avoid vignetting when using the 0.3 m mirror. The distance from the 0.3 m mirror to the target object is $d_{Mt} = d_T - d_{CM}$ where d_t and d_{CM} are the distances from the celestron primary mirror to the target and the 0.3 m mirror respectively. D_T and D_M is the diameter of the celestron primary mirror and the 0.3 m mirror respectively.

As can be seen further down the distances to the targets are 300 and 600 meter. Using these distances the needed minimum diameter for the mirror D_M, that is now 0.3 m, can be calculated using equation 42 and solving for D_M. The sizes are displayed in table 4:

Table 4: The minimum needed size that would have been needed for the 0.3 m mirror

d_T [m]	D_M [m]
300	0.33
600	0.35

This means that for the two longer distances the new 0.3 m mirror is actually to small and will act as a pupil. Measured in area at 300 m the mirror is 9.8% too small and at 600 m it is 17% too small.

4.3.3 LED target

A high intensity red LED light was put on the target (thus it became both a LED and resolution target) to focus on during night time observations and for the days when it is cloudy (which it often is in Lund). A text has also been used to see if it could be read as another option to the resolution target, the text was: "Can this be read?". The diagram for the target and the diagram for the electronics is displayed in figure 11:
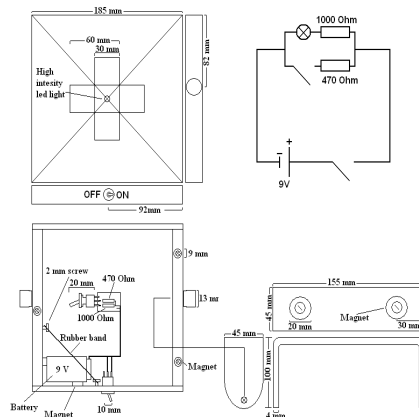
Figure 11: The LED target.

The specifications for the red LED light can be found in LEDZ [9]. Note the peak value of the LED is at 635 nm, this is the reason for the removal of the low pass filter in the setup. The spectral range of the LED is ∼600-670 nm.

4.3.4 Modified LED target

Testing other targets for the AO-setup, the top most part of the LED was cut of and a cross was cut into the now flat top of the LED. The cross was then painted black to give a sharper contrast. This resulted in a somewhat lower light emittance in the forward direction of the LED. The reason for the cross was to give the AO not only light to compensate with but also some structure.
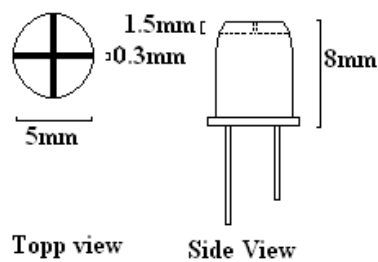

Figure 12: Modified LED light.

4.3.5 Other targets

At longer distances than to the tower of the institute here in Lund, light sources such as height warning lamps on buildings and chimneys were used. The first one was on the "Kemi Centrum" building at a distance of about 600 $\pm$ 30 m and at an intermediate distance of 300 $\pm$ 10 m there was a chimney with a height warning lamp. These types of lamps are basically strong light bulbs with red glass covers.

5   Method

The base method for this thesis consists of data gathering, data reduction and drawing conclusions from the results.

Gathering the data was much about trial and error, see what does and does not work for the equipment used. Before any real data was captured calculations where done to see if the equipment could handle the amount of light that were supposed to be gathered to get the data. These equations used are stated in section 3.6 and the results are found in section 6.1.

5.0.6   Flux calculation program

In order for the flux calculations to not take to much time, a program was created to calculate the flux with different input values. This program calculated the flux from the moon and the flux resulting from the reflection from the resolution target, using real measured flux profiles from the Sun and the albedo profile of the moon.

In addition, the program calculated the flux that would come from the LED target using an approximated spectral profile for the LED. The Solar flux profile was acquired from Wehrli 85. [15] and the Moon albedo profiles was acquired from ESA EOQ 50 GOME [2], these profile can be seen in the Appendix A, plots 2 and 3.

To get the flux in the setup from the resolution target was straight forward using the solar flux for the appropriate wavelength integration region using equation 2. To get the Moon flux the Solar flux profile needed to be multiplied by the lunar albedo profile and integrated over the appropriate wavelength region using equation 35.

The LED light flux calculations were done using equation 36.
The results from these calculations can be found in section 6.

5.1   Using the equipment

In this part a normal observation night/day will be discussed in short, pointing out the most important part. Beginning from startup, looking at how "small" calibrations are done and how the data acquisition was done and ending with shut down. Further more, an overview of how the "big" calibration was done. What is meant with "big" and "small" calibrations will become apparent when reading this part.

If more information about the calibration or running the setup is of interest the reader is referred to Appendix B; "Using and calibrating the Adaptive Optics setup", this is a step by step manual on how to start, calibrate and

use the AO-setup and the computer that collects the video data. In addition, it describes how to use the telescope controlling computer.

Both when aligning the system and during real observations the AO system and the AO controlling computer need to be started. The first thing to do is to start the power supply to the deformable mirrors. Then via the AO control program (Matlab based) apply the bias to the deformable mirrors and the tip-tilt mirror. This is to give the deformable mirrors the correct concave shape so that their focus lengths are matched to the rest of the system so that the light is sent all the way through the system to the focus plane of the WFS and the SC. For the tip-tilt mirror the applied bias gives it the correct zero position so that the light can travel through the system.

The SC control computer needs to be started in order to be able match the positions of the light from the reference and calibration arms in the FoV of the SC and at the same time have the FoV of the WFS looking correct, more on this in later and in Appendix B. This is needed both when aligning the setup and for normal observation calibrations. The SC control computer needs to be able to collect data.

The test light at the end of the calibration arm and reference arm need to be started both when aligning the system and for normal observation opportunities.

5.1.1   Aligning the system

The room where the AO-setup is placed is also used for other observations that require the siderostat. Because of the limited space available and the need for using the siderostat for solar observations, a part of the AO-setup is mounted on an optical breadboard that can be lifted. All the components of the AO-setup that comes before the first deformable mirror, including the calibration arm, are mounted on this optical breadboard. Thus, whenever the setup room is used for other forms of observations this part is elevated. When the breadboard is lowered again the system is in need of a complete recalibration.

The name of the game when aligning the system is to get the test light from the calibration arm focused in the center of all of the WFS's subimages and to match the reference arm light position in the FoV of the SC to the position of the light from the calibration arm. These two criteria must be simultaneously fulfilled. The second criteria is self explanatory, the first is not. Looking at the monitor for the WFS and having activated the Matlab program "camera show" a window with a grid is shown and beside the grid is a field where the Hartmann vectors for the WFS is shown. The light dots created by the calibration arm are to be lined up so that each intersection in

the grid has one light dot, see Appendix B for more information.

There are only six things that should not be changed with the setup, the placement of the celestron, the two positions where the calibration arm and the reference arm enters the main structure of the AO-setup and the mirrors. All other parts can be moved back and forth along the guide rails, moved up and down, moved to the sides and in some cases be tilted to give the best possible result. However the movement needed is very small, at maximum one or two millimeters for any one part.

The whole process is trial and error, going from one part to the next and back again, which can take several hours. What the effects of moving each part has can be found in the Appendix B.

5.1.2   Typical observations and small calibration

During a typical observation session the calibration should go fairly quick if the system alignment is done well. The step by step process of the calibration can once again be found in Appendix B but the main important parts are discussed in this section.

The grid pattern has to be correct and to match the light point coming from the calibration arm and the light coming from the reference arm in the FoV of the SC. However if the system was aligned correctly it should only be a matter of looking to see if it is still good.

For the AO to work the system needs a reference image. The first step to get this is to turn off all the light in the setup room, including the monitors, or covering the WFS and taking a bias picture with the program "AO menu" under the function "calibration". By introducing the reference arm into the main structure of the AO system and taking a reference image the system creates the needed image. This entire reference image (all the subapertures included) can be compared via cross correlation to the following acquired images, for when the AO is in use, to drive the tip-tilt mirror.

The next thing the AO system needs in order to work is an response matrix that determines how the tip-tilt mirror and each of the actuators of the second deformable mirror respond to changes in the light pattern. This is assuming that only one deformable mirror is used to compensate for the atmospheric turbulence, as is the case here. Before the response matrix can be acquired, the reference arm needs to be removed and the calibration arm needs to be introduced. This is done by turning on the power to the motor that is connected to the mirror that is lowered into the F/11 spot. The light from the calibration arm should be seen in SC monitor, this light should be at about the same position that the reference arm light was if the system alignment is done well. The response matrix can now be acquired by first

pressing the "tip-tilt poke" and then pressing the "actuator poke" after the tip-tilt mirror has been poked. The movement of the of the Hartmann spots are stored for the tip-tilt mirror. The actuators of the deformable mirror are poked one by one in a outward spiral pattern and the information about the response of the Hartmann spots are stored in the interaction matrix containing information of all actuators.

The next step is to set which number of singular-value decomposition (SVD) modes that is to be used. A reconstructor is formed from an interaction matrix using SVD and rejecting small singular values. This is because small singular values in the interaction matrix results in high sensitivity to noise in the reconstructor matrix (pseudo-inverse). The reconstructor determines how the sensor measurement (WFS measurements) should be converted to actuator poke signals. A suitable number of SVD mode is between 3 and 25 depending on the coherence length and coherence time, higher values for longer coherence lengths and coherence times. If the SVD number is set to 3, only tip-tilt is used.

After this, a specific subaperture is chosen for the other apertures to be compared to. If no subaperture is manually chosen, then number twelve is the set standard. What is wanted here is a subaperture with a high contrast. By doing cross correlation of the different subapertures with respect to one preset subaperture the shifts are calculated and the reconstructor is used to calculate actuator commands. This is what drives the deformable mirror.

The final thing to do is to test the calibration. Activating "./mcontrol" (see Appendix B) should turn this blob into a more or less aberration free light dot that should put the light dot at the same position as the reference light was, if it was not already. If this is not the case then everything after pressing the "tip-tilt poke" should be redone. If that does not work, then the system needs to be realigned.

Now the calibration for the AO system is done and the light from the target source can be introduced. Opening the wall lid is the first step so that the light can enter from the outside.

5.1.3 Locating the targets

To get the light from a target into the AO-setup a siderostat was used as already explained. This siderostat is controlled with a computer that can either track an object on the sky or the motors of the siderostat can be given commands directly, as is the case in this thesis project, where the targets are stationary. The targets used during this thesis where the LED/resolution target explained in section 4.3.4 and the height warning light explained in section 4.3.5. The LED/resolution target was placed on the old water tower that is a part of the institute. To get this distance (70 m) blueprints for the astronomical institution building in Lund was acquired from Torbjörn Wiesel. A representation of the astronomical institution with focus on the siderostat and the tower where the target was placed can be seen in figure 13:
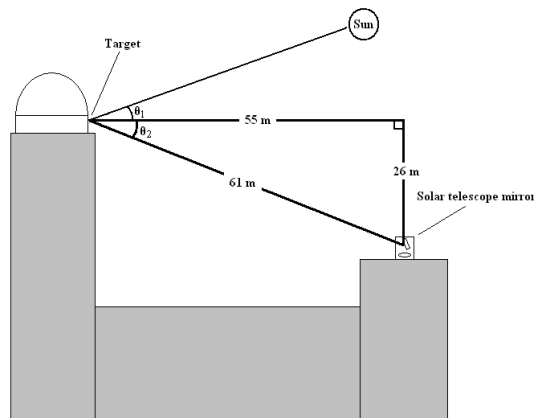
Figure 13: A representation of the siderostat/tower setup with distances and angles between the Sun, target and the mirror.

In the image the target is placed vertically. The angles between the Sun and the target normal, θ_1, and between and the first mirror of the siderostat, θ_2, are displayed.

The horizontal distance from the place where the siderostat is to where the target was placed was measured with a ruler and rescaled to real distance of 55 m. The difference in the floor levels on the balcony of the tower and the floor of the place where the siderostat were given in the blueprints as height above sea level, to this was added the hight from the floor to the center of the siderostat mirror and from the balcony floor to the height for where the resolution target were later placed. The total height difference was 26 m. Using simple trigonometry the distance from the siderostat primary mirror to where the target would later be placed was calculated

to $\sqrt{26^2 + 55^2} = 60.8$ m. This value was checked by Torbjörn W. with a laser measurement tool, that gave the distance: 61.3 m. The difference is negligible.

Neither of the two siderostat mirrors have any power, i.e. they are plane mirrors. The first mirror that has any power is the primary mirror in the celestron. To get a value that can be used to calculate the size of an object at the closest distance that will be used, the distance from the siderostat primary mirror to the celestron's primary mirror needs to be added to the 61 m. The distance from the center of the main mirror of the siderostat to the center of the secondary mirror of the siderostat is 0.86 m. The distance from the center of the siderostat secondary mirror to the center of the outside of the celestron secondary mirror holder is about 5.6 m, the two distances just mentioned was measured by Torbjörn W. The final distance between the two mirrors of the celestron is 582 mm according to Knutsson [8]. Adding these distances and with some room for errors gives 7.3 m. This distance is important and is used when doing the flux calculations. Thus the shortest distance for which the setup will be used is $61 + 7.3 = 68.3$ m (approximated to 70 m).

The airplane warning lights are located on the "Kemi Centrum" building in Lund and on a chimney just northwest of Lund observatory. Kemi Centrum is located about 600 meters from Lund observatory and the chimney at about 300 meters. These distances were approximated using a map of Lund.

The tower target:

Due to limitations of the siderostat, targeting the tower needed to be done with care in order to not ruin the equipment, thus some calculations were needed. Measurements were taken from close proximity to the siderostat to about where the target was suppose to be on the tower. One axis was given in the horizontal frame: Azimuth $A = 74^o$, and one was give in the equatorial frame: Hour angle $H = 32^o$. The siderostat uses an equatorial reference frame with declination, δ, and right ascension, Ra, as input values. Thus a translation from the two frames to the useful frame is needed. The given values translates into:$\delta \approx 19^o$ and $Ra \approx 61^o$. To do this translation the following equations were used:

$$\delta = sin^{-1}(sin(\phi)\sin(a) + cos(\phi)cos(a)cos(A)) \tag{43}$$

ϕ is the altitude to the celestial pole, in Lund this is $\approx 35.4^o$. a altitude of the target. The relation between the equatorial and horizontal frame can be seen in figure 14, see Scott [12]:
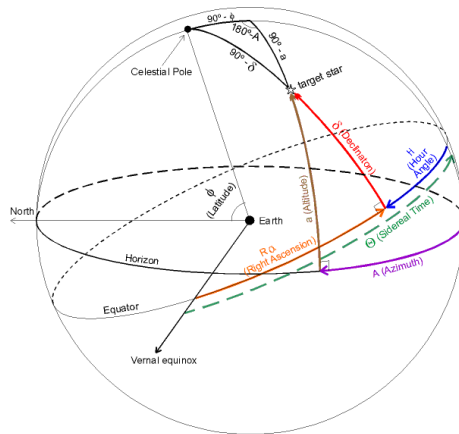
Figure 14: Relationship of Equatorial and Horizontal Coordinates.

The motors that moves the siderostat primary mirror uses a computer program that uses input in radians. To get the declination and right ascension in radians they are multiplied with $\frac{\pi}{180}$ and since the incoming and outgoing angles on the telescope mirror are the same, these values has to be divided by 2, thus: $\delta \approx 0.166$ rad, $H \approx 0.532$ rad, to find the target on the tower. Beyond this, small adjustments, of the size 10^{-4} rad, were needed to get the target into the FoV of the WFS and the SC, since the FoV is 14.8 arcsec.

Targets in the new 0.30 m mirror:

The position of the newly added 0.3 m mirror was basically straight in front of the siderostat, thus the siderostat would not come close to the primary mirror movement limitations, i.e. the holder for the siderostat primary mirror would not hit the safety beams that are around the siderostat. To find the 0.3 m mirror with the siderostat, trial and error was used with some qualified assumptions. The rough position of the 0.3 m mirror is $\delta \approx 0.122$ rad and $H \approx -0.2$ rad. Using this mirror, objects further away could be used, the only thing needed was to redirect the 0.3 m mirror. To find the objects in the field of view of the cameras and WFS only small corrections were needed for the siderostat primary mirror. Objects further away were located in the 0.3 m mirror by looking in the light path just in front of the celestron and seeing that the object became visible in the reflection at about the center of the 0.3 m mirror.

5.1.4 Data capturing

When the siderostat has been correctly aligned with the AO system target, the celestron needs to be focused to get the smallest possible light dot. This is done by turning a screw that moves the primary mirror of the celestron.

Now that the calibration, targeting and focusing is done the next step is the actual data gathering. The data is gathered in the science focus using the SC. The program used is "QCapture PRO" from QImaging. This is the controlling program for the SC. The program can be set to either capture images or video files.

After some initial trials the video capture files got a "standard" that seemed to work well. Each video file consisted of 450 frames. When the AO could be used the first ∼150 frames are before the AO is turned on. The next ∼150 frames are when the AO is turned on and in the last ∼150 frames AO system is turned off again. When the AO could not work, all the 450 frames was captured without AO. The frame capture size does not matter as long as it is larger than the cropped size of the incoming light (by the field stop) that is fitted to the size of the subaperture of the WFS. In the SC this is about 140 by 140 pixels. The calculation to this limitation was done in section 4.2.3.

The reason for the three steps of AO usage in the video capture is firstly to see how the AO affects the image and secondly to see if the AO has worked properly. There should be no difference in the r_0 measurements between before and after the AO is used if the system is well calibrated unless the actuators are driven into saturation.

The minimum time lapse between each frame is limited by the SC internal speed which is 1 μs, see QImaging [11]. There was some experimenting with the exposure times and the time lapse between the captured images. A long exposure time has the effect that is smears out the light source. This is not good since this hides the effects of the image shift. The time lapse between the frames is important, since the individual frames should be uncorrelated to get an unbiased result. Having the frames correlated gives a smaller relative movement and in extension the coherence length will seem longer than it is. The exposure time for each frame needs to be shorter than τ_0 for the analysis of the frames to get r_0 values that are not affected by spot-smearing which results in overestimating the coherence length. The time lapse between frames needs to be longer than τ_0 for the same reason. The exposure time is set between 2-10 ms according to the calculations done in 3.3 depending on the weather conditions, the time lapse was set to between 25 and 50 ms.

For each observation session around eight sets of 450 frames were captured and the average length of one session took about three hours.

5.2 Computer programs and data reduction

Several programs were created to calculate the incoming flux, coherence length, coherence time and the error or variance estimates of the previous two. These programs were all created in Matlab by the author with the exclusion of the subprogram called "barweb" which is free to download from MathWorks and was only edited by the author of this thesis. "barweb" creates bar-plots with attached uncertainty or deviation values.

5.2.1 Center of gravity tracking by intensity

The first attempt at creating a image analysis program did work and was used early during the thesis, however the program was very slow. The program finds the light source center in each video frame by searching for the area with the same size as the light source with the highest intensity. These positions are stored and the shift is then calculated between frames. These shifts are then recalculated from unit pixels to radians as described in section 3.2. Finally r_0 was calculated using equation 8. In this program a part was included to calculate a rough coherence time value. By using equation 15 and inserting the measured wind speed, the rough wind direction in relation to the propagation direction of the light and the coherence length, the coherence time was estimated.

5.2.2 Center of gravity tracking by fft

Since the previous mentioned program was quite slow another program was created using Fourier transform. The program starts by selecting the frame with the highest contrast and uses it as a reference frame. The contrast is calculated for each frame by dividing the variance of the intensity with the mean intensity. The reference frame is then Fourier transformed and correlated by multiplying it with the complex conjugate of the Fourier transform of all the other frames individually. Taking the inverse Fourier transform of the correlation matrix and extracting the center position of the images gives the shift of the light source in the image in unit pixels, i.e it finds the peak position of the correlation matrix. These shifts are used together with equation 20 in section 3.4. Converting the values to radians and from there getting the r_0 and τ_0 values was done just as in the first center of gravity program.
This program gave the same results as the first center of gravity program but was about 600 times faster.

Important to note is that the resulting coherence length is highly dependent on the frames used to get the coherence length. Each set contains 450

images, divided into three groups containing about 150 frames each.

Since the AO control system is not connected to the data gathering programs used in this thesis, the sets are only roughly 150 frames. The first group is when the AO has not been turned on, the second group is for when the AO is running and the final group is after the AO has been turned off again. It is hard to see by ocular inspection which the frames belong to which group. The "border frames" around 150 and 300 can vary with $\pm 4 - 6$ depending on factors such as integration time and the concentration of the person sitting and conducting the observations (the author).

Because of this sensitivity to "border frames" the program varies the number of frames and calculates a total of 110 coherence length values for each group of frames. The value 110 comes from how big the uncertainty in starting and stopping the AO system, starting in the range 146-156 and stopping in the range 295-304. In the end storing the values that complies to the highest coherence length value for the second group (with the AO on). As long as the higher and lower "border frame" is not always the same (e.g. always 295 and 304), the frames in the second group should be the frames for when the AO is turned on.

Calculations of the variation of $< \alpha^2 >$ were included into this program since most scientific work has some form of uncertainties that are either due to the equipment, mathematical calculation precision or other variables. The variation values are acquired by following the calculations in section 3.5.

The results were checked by using equation 27. If the result differs from $\frac{1}{n}$, then there is some error source in the measurements. If this difference is small, then the method to get coherence length is robust.

6 Results and conclusions

In this section the results of all the calculations and measurements will be presented. Further more, the conclusions obtained from the results are discussed in this section.

6.1 Flux integrations

Using the equations for flux integration in the theory section, equations 35-37, the number of photons hitting the WFS and the SC during some time unit can be calculated for the Moon, the LED and light coming from the Sun reflecting of the target and reaching the setup. The Moon is used to check the calculations done in this thesis against Knutsson [8].

The number of electrons in the detector resulting from each photon impact is just a case of multiplying with the quantum efficiency, Q.E, of the WFS ~ 0.7, see Knutsson [8], and for the SC ~ 0.7.

A comparison to the results in Knutsson [8] is of interest to validate the values acquired in this thesis. In Knutsson [8] the value is calculated for the WFS and there were a bandpass filter used that excluded all wavelengths except for 700-800 nm and the beam splitter only sent 20% to the WFS (90% for this thesis). The result obtained in Knutsson [8] was 580 electrons per pixel per millisecond. Comparing this to the value calculated in this thesis of 785 photons, which turns into 550 electrons per pixel per millisecond with the Q.E of the WFS. Calculated for the setup arrangement used in Knutsson [8]. This difference is small and due to a small difference in approximating the lunar albedo and solar intensity. The results of these calculations can be seen in table 5 and 6, the first for the WFS the second for the SC, for the case of the target at $\sim$70 m.

In the following tables STM1 and STM2 are for when the target is placed face on with respect to the siderostat primary mirror and when the target "face" is vertically placed. This means that the angles θ_1 is $\sim 25.3^o$ when θ_2 is $\sim 55.6^o$ or θ_1 is 0° when θ_2 is $\sim 80.9^o$. 80.9^o represent the absolute highest position the Sun can have in Lund during a full year with respect to a target positioned as described above. The $\theta_1 = 0^o$ case gives an absolute max that is useful to compare with. Theoretical in the sense that if the Sun would actually be in that position it would be well below the horizon.

A short reminder: integration region is 200-1100 nm, the integration time is 1 ms, and the Moon and resolution target takes up the full field of view (14.8 by 14.8 arcsec.). The LED has a diameter of ~ 11.4 arcsec at 70 m.

Table 5: WFS list of captured photons and generated electrons

WFS	γ	e^-
n_{moon}	13168	9218
n_{STM1}	10065	7045
n_{STM2}	32505	22753
n_{LED1}	3575	2502

Table 6: SC list of captured photons and generated electrons

SC	γ	e^-
n_{moon}	628	440
n_{STM1}	451	316
n_{STM2}	1516	1061
n_{LED}	201	141

As can be seen there are roughly 0.5-1.5 times as many photons reaching the detector per millisecond for the STM in comparison to the Moon. Hence there are roughly 0.5-1.5 times as many electrons generated for the STM in relation to the Moon.

The WFS's and the SC's full well capacity are given in number of electrons generated for each photon impact and is 215 ke^-, for the SC this is 22 ke^-. Comparing this to the number of electrons that will be collected under favorable conditions and no gain used, $\sim 23ke^-$ per ms for the WFS and $\sim 1.5ke^-$ per ms for the SC. This means that there will be no need for a ND filter during the data collecting for up to ~ 10 ms exposures for the WFS and ~ 15 ms exposures for the SC if the sky is clear. If the sky is covered or semi-covered with cloud it can be substantially longer. The filters are needed during day time observations in any case, since the monitor camera is saturated much earlier than the other two cameras, but the filters are removed during data collecting.

6.2 τ_0, r_0 and AO correction

The plots created for this thesis use data gathered by the SC. A maximum gain of 45 times the incoming value could be used for the SC to get better results. The gain used was determined on what was needed during each observation opportunity and should have no effect on the final results if used sparsely. Gain is defined as electrons per digital unit from the AD (analog to digital) converter. If the gain is large, quantization noise may dominate. High noise data from observations has been discarded.

6.2.1   Description of the plots

Different types of plots have been created to study different aspects of the atmosphere and how the AO system affects the seeing. In Appendix A the plots on the left from 6(a) to 16(b) are created using the coherence length calculations, described in section 3.2. In these plots the y-axis is coherence length in units of meters.

Using information about the winds speed perpendicular to the observation direction and equation 15, the coherence time plots on the right are acquired, based on the coherence length plots. The y-axis in these plots have coherence time in units of seconds. The x-axis differ for different plots and will be described in deeper detail shortly. All the plots have variance values attached to the bars, the calculations to get these can be seen in section 3.5.

There are several types of coherence length/time plots, that shows different aspects of interest. The coherence length plots and their corresponding coherence time plots are placed together.

1. Plot 4 in Appendix A, shows a standard observational opportunity. During one standard observational opportunity several (normally eight) data sets were captured, each set having 450 frames. The sets are displayed in the plots according to the order in which the data sets were captured. One set contains 3 different bars. The three bars represent three types of coherence values, these are for "before" (turquoise bars), "during" (purple bars) and "after" (pink bars) the AO was in use. Set number six is uncharacteristically high in comparison to the rest, which are at normal and expected levels. This might be due to the wind being temporarily calm. There are also sets with the "before" and/or "after" bars are larger than the "during" bar. This is likely due to some temporary wind gust or fluctuations in the power supply. From the point 4 in this list and onward the bad data sets and the sets where the "during" values are lower than either of the other two

have been removed. Thus the plots only show data where the system is functioning properly.

2. Plot 5, shows what happens when the setup has been badly focused or when the integration time is to long. The different sets goes towards one single value. This is due to the image becoming smeared out over a large area. Thus any variation is smeared out and the coherence length/time value goes towards a non zero constant value. This constant value is related to the precision in the measurements of $< \alpha^2 >$ and can thus never become zero. Such plots are all removed from the coherence length/time analysis because all the information about the coherence length has been lost.

3. Plots 6(a)-15(b) show the individual observation opportunities. These are sorted firstly by the distance to the target, then by daytime or nighttime and lastly by date. There are plots that have less than eight data sets because less sets were captured.

   The plots that do not have three bars for each data set are for when the AO system was not working properly for one reason or another. When the AO could not be used (i.e. at 600 m) there are only bars that show "before" the AO is turned on.

   When the AO has been used and is turned off, the voltage pattern is left on the DM. This means that some shift is corrected for in the "after" bars. Thus both the "before" and "after" bars could be called true coherence length since they only show the effect on the shift that is caused by dynamical effects such as the air turbulence. The "during" bars are modified coherence lengths and represent how well the system can compensate for the air turbulence in relation to the other bars. If the system is working correctly and with good weather the "before" and "after" bars should have about the same height and the "during" bars should always be higher than the other two bar types.

4. Plots 14(a)-16(b), show all the data that have used AO for all distances. The data has been sorted according to the distance to the target. For each target distance the "before", "during" and "after" have been separated and then sorted according to the "before" part, which is sorted according to its coherence length/time. This means that the "before" bars will be sorted nicely and the other two will show the equivalent "during" and "after" bars. Neither of the two should be perfectly sorted. It might however be possible to see an overall trend in some of the plots.

6.2.2 The information in the plots

Coherence length and coherence time:

1. At 70 meters it can be seen from the plots 6(a)-10(b), that the coherence length that the system can handle is shorter than the expected 0.05 meter value, especially during night time with the LED light. There are definitely improvements of the image, the "during" bars are for the most part the highest bars with the two other bar types being roughly the same as they should. Improvement meaning that the "coherence length" goes up, due to that the center of gravity of the light in the captured image data is being displaced less.

   At 600 meter, plots 11(a)-15(b) show that this is around the distance limit that the setup can handle the turbulent atmosphere. The boundary seems to be at around a coherence length of 0.015 m for where the tip-tilt stops working properly. Going from higher to lower coherence length the AO will work for fewer and fewer of the higher order aberrations. Comparing the plots 6(a)-10(b) to the plots 11(a)-15(b) the ratio of the coherence lengths are about one third to one fourth. This is what is expected using equation 7 depending on the wind and how well the setup has been calibrated at the time of the observation.

   The average exposure time for a data set is about half a minute (450 frames with 3 ms exposure time and 50 ms between exposures). During this time the atmosphere clearly fluctuates greatly. The coherence length can vary by a rough factor of two. From time to time wind gusts come, greatly influencing the measurements by reducing the coherence length, in many cases to below what the setup can handle. There seem to be an low order fluctuation in the coherence length on the same timescale as an entire data gathering opportunity, i.e. eight data sets or about 10-15 minutes. This conclusion is drawn from the wave like profile of the some of the data gathering opportunities such as plot 6(a) and 8(a). To really determine if there is a low order fluctuation in the coherence length a longer exposure of several tenths of minutes would be required and dividing that into smaller bins of the size of one minute to a few minutes.

2. For the plots 14(a)-16(b), the "before", "during" and "after" plots do not match perfectly (as expected) due to the turbulent nature of the atmosphere. It is however possible to see the basic structure of the "before" plots in these plots.

It can be seen in these plots that the system is capable of handling turbulence with coherence lengths down to around 0.01-0.015 m. Probably only tip/tilt is improved. There is an important point that needs to be taken up about short coherence length limit. At these coherence length the exposure time of 3 ms is likely to long according to what can be seen in plot 14(a). This would imply that the coherence length is over estimated. It might also be that the wind speed or wind direction has been wrongly estimated. This would imply that the setup can be used below a coherence length of 0.01 m. At this length scale higher order fluctuations cannot be corrected because the subaperture which has a size of about 0.07 m when it is projected to the entrance pupil. This can be tested by doing more observations with integration times shorter than 1 ms but it would not be possible to inspect the gathered data visually because the image is too faint for the human eye. The WFS integration time is set to 2 ms and thus needs to be changed to do observations with these integration times. The optically inspection can be helped by having longer integration times.

The longest coherence length that is acquired at 600 meters is about 0.075 m, at 70 meter this is about 0.105 m during day time observations. Acquired for when the weather is good and the atmosphere is relatively calm.

The coherence time plots shows a greater relative span for the in comparison to the coherence length, i.e. a span of 1 ms to 19 ms in comparison to 0.01 m to 0.10 m. This would suggest that the wind is not the most important parameter at the lower end of the coherence lengths. The average trends going from "before" to "during" and "after" is more apparent in the coherence time plots than in the coherence length plots, this is due to the greater relative span that the plots cover.

The average values are about 0.051 m and about 7.07 ms for 70 m and about 0.03 m and 5.3 ms for 600 m before AO is used.

6.2.3   A lamp at 300 m

There were observations made at 300 m. The target was of similar type as the target at the 600 m distance, an airplane low level warning light. However, the light at 300 m was larger than the light at 600 m, this made it impossible to use the light as a point source. The 300 m had a frequency that was longer than 10 ms, thus making any determination of the atmospheric coherence length impossible. The flickering of the airplane lamp disappeared at about 20 ms, thus it is likely that the lamp had a frequency of 50 Hz.

However, there where a metal grid covering the lamp that was visible to the system and human eye. Because of this it was attempted to see if the system could do anything about the observed image. Using only tip-tilt the system seemed to stabilize the image to some extent, however having a hard time doing so. Figures 15(a)-15(c) below shows what the lamp and grid looks like with the AO both on and off. It is hard to see any improvements in the images, but the "during" AO image has somewhat smaller lines (the brighter parts) than the other two. Figures 15(a) to 20(c) have been contrast enhanced to make them easier to see on printed paper.

(a) "Before" AO   (b) "During" AO   (c) "After" AO
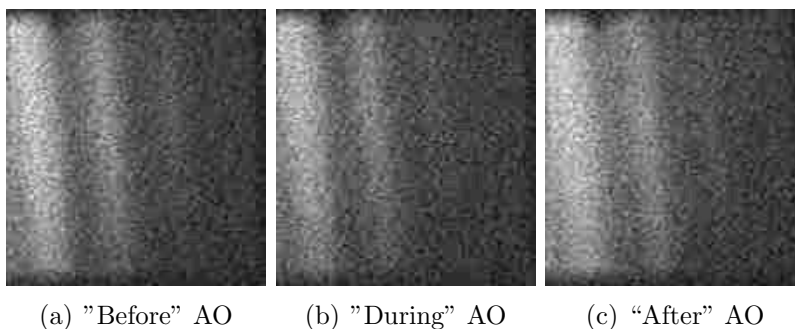
Figure 15: The lamp and grid at 300 m.

6.2.4   Observations of the resolution target and a text

Resolution target

As previously mentioned, a resolution target has been observed at 70 m. Even though the SC has a resolution that is high enough to resolve the finer details, the air turbulence and the best possible correction made by the AO system will not allow it. Even at optimum focus (or at least very close to it) the image quality for the resolution target was very bad. The contrast became too low, thus the program that was used to analyze the data could not detect any improvements.

Because the resolution target was not a point source the reference used was the one with multiple dots. Using higher order AO did not work, just as with the lamp and grid at 300 meters. Using only tip-tilt gave some visible improvements, though only limited that could be seen by eye. Having the exposure time at 3 ms, it was very hard to see if the image got better or not.

The following three images show the results of the observations of the resolution target at 3 ms exposure times:

(a) "Before" AO   (b) "During" AO   (c) "After" AO
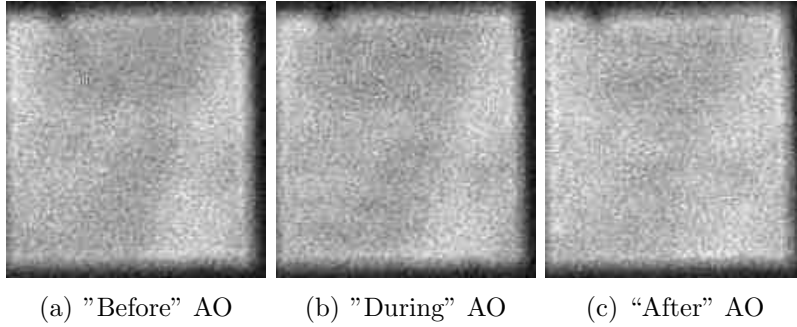
Figure 16: The resolution target at 70 m with 3 ms exposure time.

The following images shows the "before", "during" and "after" images of the resolution target at 5 ms exposure times.

(a) "Before" AO, 5ms   (b) "During" AO, 5   (c) "After" AO, 5 ms
ms
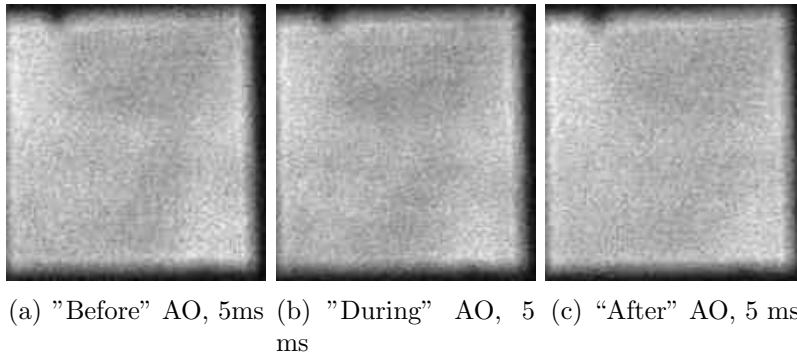
Figure 17: The resolution target at 70 m for 5 ms exposure times.

It is a bit easier to see the resolution target than for the 3 ms exposure but it is still hard. Going on to 20 ms exposure it is easy to see the resolution target but the image is very blurry. This is likely due to a combination of seeing and the unstable power supply of the deformable mirrors and tip-tilt mirror, which at times dipped to zero voltage.

(a) "Before" AO, 20 ms   (b) "During" AO, 20 ms   (c) "After" AO, 20 ms
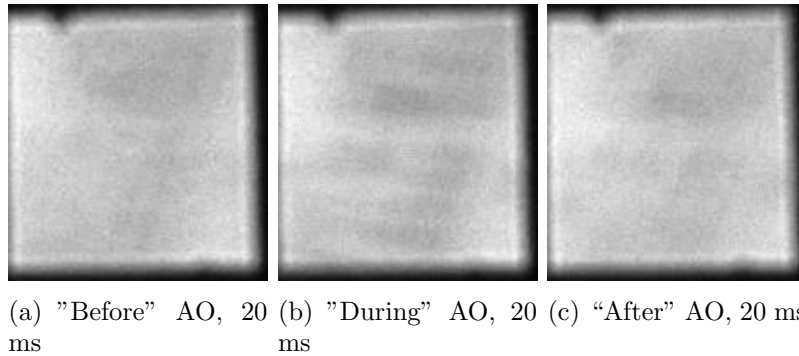
Figure 18: The resolution target at 70 m for 20 ms exposure times, This was captured on a less than perfect day so there was very little risk of saturating the SC.

At longer exposure times it is easier to see the target but any information about the coherence length is lost as explained earlier.

A short text

A text was also studied, which said "Can this be read?". The size of the text was 10 pt and 12 pt. The entire sentence could not fit into the FoV of the setup but complete individual words were visible. Just as with the resolution target and the lamp and grid at 300 m, the coherence length of the atmosphere could not be acquired due to image quality or long exposure times. There were however clear improvements to the image, see figures 19(a)-20(c), when using just tip-tilt and having used the multiple point source reference when calibrating the system. The following images of the text was captured during a particularly sunny day.

(a) "Before" AO   (b) "During" AO   (c) "After" AO
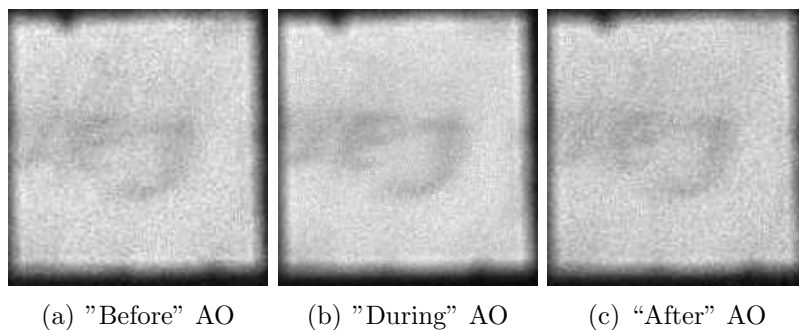
Figure 19: The text "Can this be read?" at 70 m.

The word "Can" is clearly visible up-side-down. In the following figures "n th" (10 pt) can be seen from the first two words in the sentence and also the top part of "ead" (12 pt) from line below, which was the same sentence:

(a) "Before" AO   (b) "During" AO   (c) "After" AO
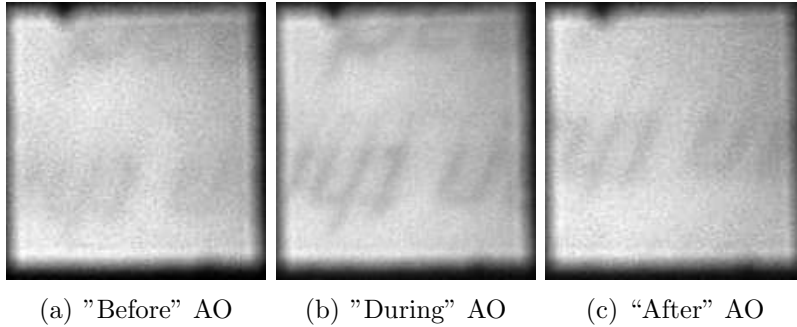
Figure 20: The text "Can this be read?" at 70 m.

6.3 Atmospheric characterization

Studying plots 6(a)-15(b), statements can be made about the atmosphere in Lund. Distance has a great effect on the image fluctuations, going from 70 to 600 m reduced the average coherence length from about six cm down to about two or three centimeters. This was expected according to equation 7.

Wind gusts decreases the coherence length greatly and abruptly. Wind gusts can be shorter than a few seconds, observed when the wind came in the short timespan when the AO system was active and effectively cut the coherence length by one half to two thirds, see plot 14(a). Short periods where the wind more or less ceased also occurred. These short periods did not last longer than 30 seconds and almost never longer than 10 seconds. It can be seen in for example plot 10(a), that the coherence length greatly improved during such an event due to the AO system being relieved of some of its workload.

There seemed to be a low order fluctuation in the turbulence, fluctuating on a timescale of about 30 seconds.

Doing observations with the wind coming more or less parallel with the observation direction greatly decreases the workload on the system due to the lower perpendicular wind speed component. The calculation for τ_0 does not hold up if the wind becomes parallel with the observation direction, but due to the determination of the wind direction with the fluctuating wind direction, the smallest angle was set to be 22.5 degrees and not zero. The equation likely under estimates the coherence time in these cases. If this is the case or not is not possible to say with the low number of data points.

6.4 Conclusions on the method

The way that the atmosphere has been analyzed in this thesis work seems to be a robust and a good way to get the coherence length and coherence time. The atmospheric coherence length behave as expected from equation 7. Using equation 27 the results were checked and it varied at most 24% (often being below 10%, for the data where the system functioned properly) form the theoretical value of $\frac{1}{n}$, which indicates that there are some error sources in the measurements but is definetley good enough to conclude that the method is sound.

6.5 System usefulness

This system was not designed to handle HAOGLA but did a fair job considering the circumstances. At 70 m the system could on a good day/night with an average r_0 of about five centimeters using AO get "r_0" values of about twelve centimeters. This can be seen in plot 6(a). Going out to about ten times that distance, 600 m the r_0 values went down to an average of about one to two centimeters which means that only tip/tilt is improved.

6.6 Recommended changes

There are several improvements that can be made to the setup that would make further observations in the horizontal plane and other types of observations easier or even possible.

1. Due to low temperatures during winter time the system stopped working. The computers that were used are not meant to be used at temperatures close to 0° C and a humidity close to or above 80%. This was very regrettable because it was expected that the atmosphere would be less turbulent since there would be less heat overall that causes the air to move. The solution to this would be to either isolate the room (would have been a bit more comfortable to work in temperatures above zero degrees Celsius during the time from fall to spring, or to have the computers controlling the setup in a rack which is climate controlled.

2. In relation to the previous point, stable computer programs would be a good idea so that valuable data would not be lost and valuable time for observation would not be lost trying to correct the problems. The programs crashed at times due to the use of an inactive subaperture being used as the reference subaperture.

3. Moving the entire setup and having a movable mirror that can redirect the light into the setup instead of having to move the setup up and down when the other setups in the room needs to be used. This would greatly reduce the work load of the person carrying out the experiments because the realignment of the setup would not need to be done as often.

   A simpler solution would be to attach a motor to the focus of the celestron telescope and to the mirror that redirects the light to the monitor camera instead of having to squeeze in between the wall and the setup, which has a clearance of ~ 30 cm, to refocus or move the mirror.

4. Changing the WFS's lenslet array to one with a smaller pitch so that the higher order aberrations can be analyzed in greater detail and corrected for more accurately. This would however increase the noise due to fewer photons per subaperture. It would also require brighter targets since there will be much fewer photons in each subaperture. Only changing the lenslet array might not be enough, the deformable mirror might also have to be changed to mirrors with actuators closer together. The program running the AO-setup might also need to be moved to a faster computer so that more information can be processed in a shorter time.

5. Having a joystick to move the siderostat primary mirror instead of having to put in numbers every time it needs to move would greatly reduce the time to locate the targets.

6. Cleaning the siderostat secondary mirror to possibly increase the image quality and inserting a heating system for that mirror so that it does not fog up (which has happened during one observation). This and the previous point are planned for.

For future work with HAOGLA, the most important change needed from this list are number 1 and number 4. Number 1 is important for the setup to function and number 4 is important to get the most out of the system performance.

7   Discussion

The method used during this thesis is robust. Filming different objects at different distances and analyzing the data by comparing all frames to one reference frame has given insight in to how the atmosphere behaves. The coherence length is around the length that is expected for a place such as Lund. The coherence length naturally changes with the distance, from about 5 centimeters at 70 m going down to an average of about 3 centimeters at 600 m. Staying close to the ground and taking account for wind speed and wind direction, equation 7 works well in the distances from about 100 m to about 1000 m.

The setup used work better than expected and was able to do AO down to the 1 cm level, which is about one fifth of what was expected but only with tip/tilt correction. This is likely an overestimation due to the too long exposure times in comparison to the short coherence length. It was probably only the tip-tilt correction that was working close to its full potential. Sadly, due to the cold weather the setup could not be used during the really cold parts of the year, where it had been expected to get very clear images with long coherence lengths. The computer's graphics card broke due to the cold weather and could not be replaced until after the winter.

With the setup as it is, going down below 3 ms exposure times is of no use since the response time of the deformable mirrors is 300 Hz.

Further work about HAOGLA should also focus on longer distances, testing to see how well equation 7 holds when only measuring r_0 without AO-correction. Another focus should be to have more images for each data set. To see if the lower order fluctuation proposed in this thesis really exists.

With better equipment HAOGLA might work well up to 1.5 or 2 km at most. This is far below what would be needed for astronomical purposes such as studying stellar object close to the horizon. This is due to the low number of incoming photons from the potential targets.

With a fully functioning AO-setup having longer exposure times should work well as long as the coherence time allows it. This would also be an interesting aspect to test if future work with HAOGLA is done.

The low amount of incoming photons is the largest hinder for HAOGLA. Another problem for HAOGLA is the actuator speed on the deformable mirrors. More and faster actuators on each deformable mirror would be needed to make HAOGLA work well. This would only be needed if the target light source sends out enough photons. A good light source would be a high powered laser. With this combination HAOGLA might become useful.

Acknowledgments

I would like to give thanks to my two supervisors, my supervisor Torben Andersen co-supervisor and Mette Owner-Petersen for all the guidance during the project. For great support with the experimental setup and work aid I would like to thank Torbjörn Wiesel, Majid Ale-Ebrahim and Ahmad Darudi, without whom I would not have come as far as I did. Furthermore, thanks to Hampus Nilsson for fixing many of the computer related problems encountered during the thesis.

For helping me with some programming and all around nice work breaks I give thanks to Fredrik Windmark, Hannes Jensen and Tobias Albertsson. Finally I thank the rest of the astronomical institute for creating a stimulating working environment.

References

[1] e2v technologies. —, `http://www.e2v.com/assets/media/files/documents/imaging-space-and-scientific-sensors/42-39-01.pdf`

[2] ESA EOQ 50 GOME. 1996, `http://esapub.esrin.esa.it/eoq/eoq52/dob52.htm`

[3] Esposito, S. 2007, Basic Concepts and Parameters of Astronomical AO Systems, P.45-78 (Springer)

[4] Fried, D. L. 1966, J. Opt. Soc. Am., 56, 1372

[5] Fried, D. L. 1990, J. Opt. Soc. Am. A, 7, 1224

[6] Greenwood, D. P. & Fried, D. L. 1976, J. Opt. Soc. Am., 66, 193

[7] Hardy, J. W. 1998, Adaptive Optics for Astronomical Telescopes (Oxford University Press, New York, NY, USA)

[8] Knutsson, P. 2008, Experimental Adaptive Optics; A test facility for adaptive optics on a small telescope (KFS AB, Lund 2008)

[9] LEDZ. 2008, `http://www.kjell.com/filarkiv/SUPPORTPDF/81-90/90/90587/90587.pdf`

[10] Masciadri, E., Stoesz, J., Hagelin, S., & Lascaux, F. 2010, Optical turbulence vertical distribution with standard and high resolution at Mt. Graham

[11] QImaging. —, Rolera-XR, High-Preformance Near-Imfrared IEEE 1394 Firewire Digital CCD Camera, `http://www.leedsmicro.com/pdf/Rolera-XR.pdf`

[12] Scott, R. L. 2009, Figure 2.6 - Relationship of Equatorial and Horizon Coordinates, Cayote Gulch

[13] Tatarski, V. I. 1961, Wave propagation in a turbulent medium (McGraw-Hill, New York, NY, USA)

[14] Valley, G. C. 1980, Appl. Opt., 19, 574

[15] Wehrli 85. 1985, The 1985 Wehrli Standard Extraterrestrial Solar Irradiance Spectrum, `http://rredc.nrel.gov/solar/spectra/am0/wehrli1985.new.html`

Appendix A.

Integration time

The following plot shows the maximum integration time that can be used and still keep the information about the coherence length of the atmosphere. The seven lines, 0.01-0.13, represents different coherence length. The x-axis have wind speed in m/s and the y-axis shows the integration time in seconds.
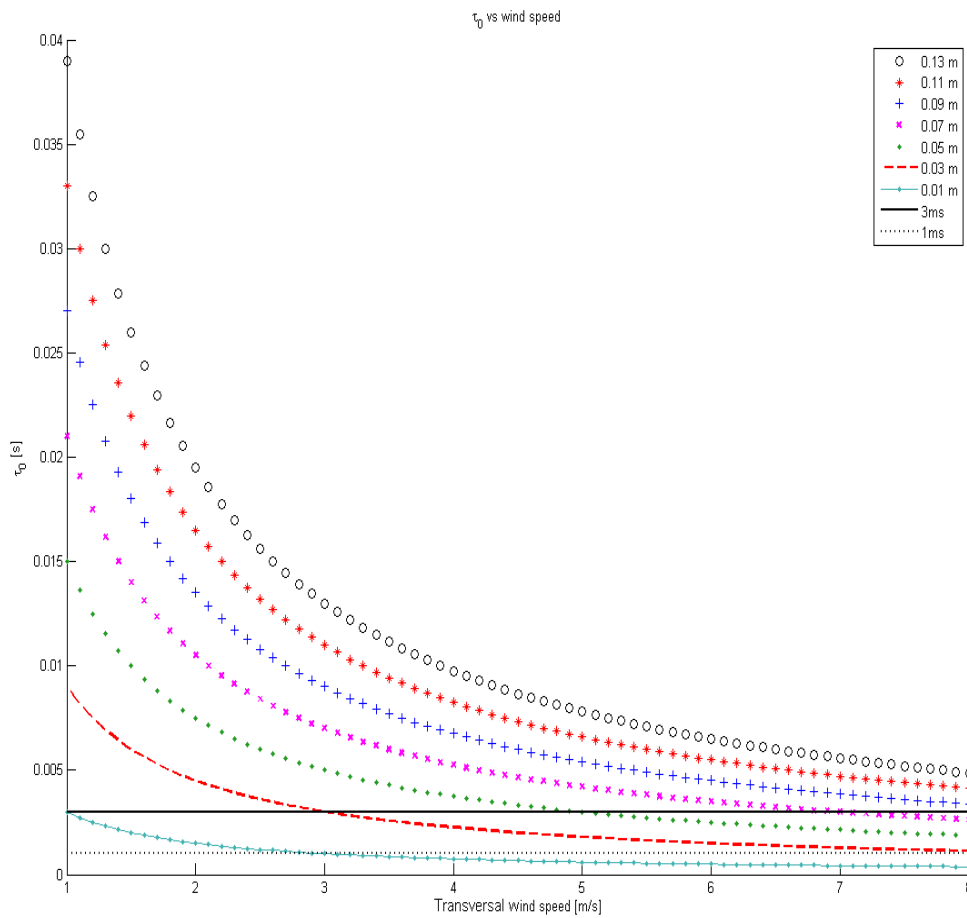
Figure 1: Integration times for different coherence lengths at different wind speeds.

Flux plots

This part contains plots representing the flux of the Sun, Moon and the LED. A plot of the Moon albedo is also shown.

(a) 200-500 nm
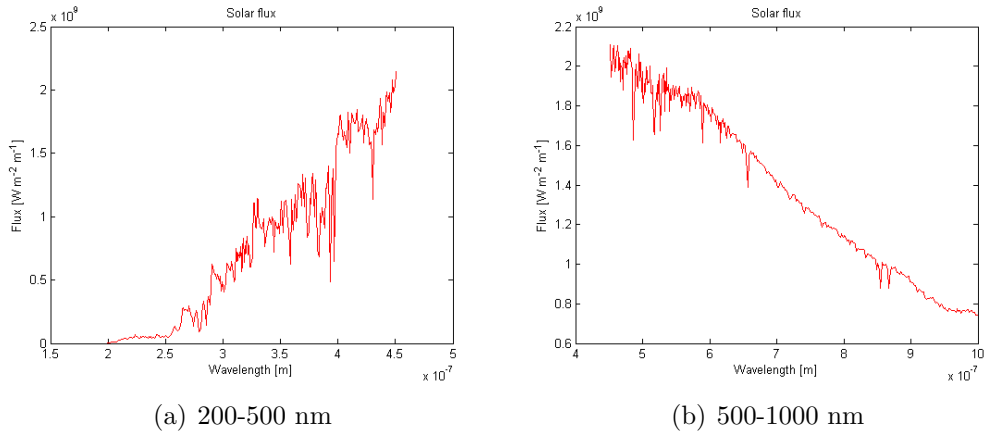
(b) 500-1000 nm

Figure 2: The Solar flux from 200-1000 nm.

(a) 200-500 nm

(b) 500-1000 nm
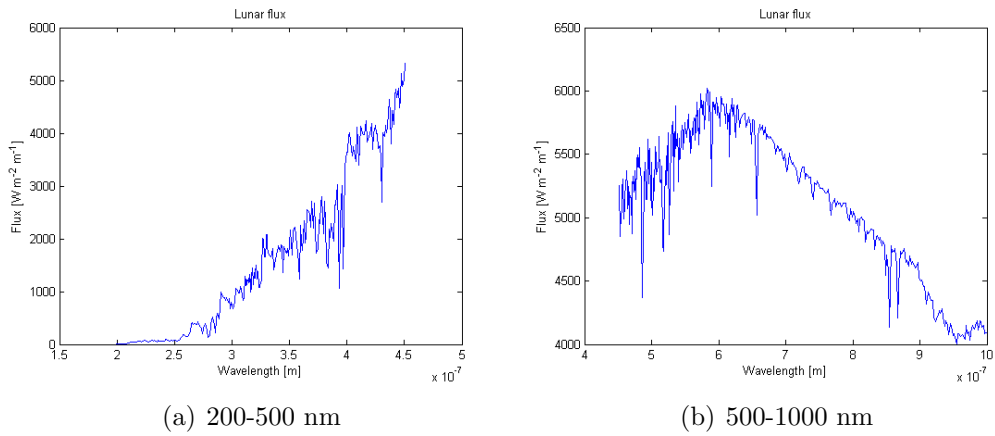
Figure 3: The Lunar albedo from 200-1100 nm.

Coherence length/time plots

This part has the coherence length and coherence time plots described in the thesis. These plots have coherence length in units of meters on the vertical axis.
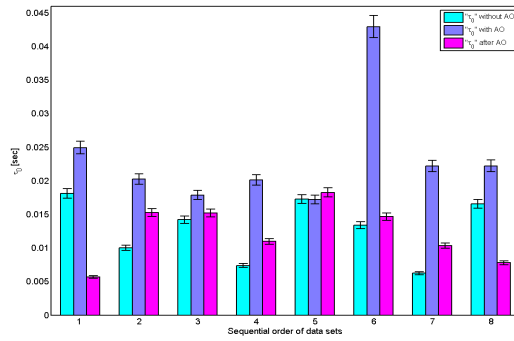
Figure 4: Coherence length plot with the sixth set being suspiciously higher than the rest and set five having lower "during" value than the "before"/"after" values.
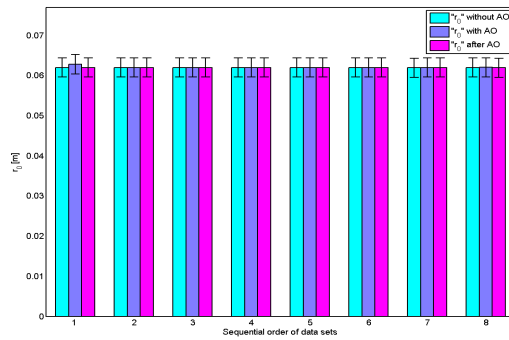
Figure 5: Example of a coherence length plot with either to long integration time or a badly focused setup.

70 m, Day time
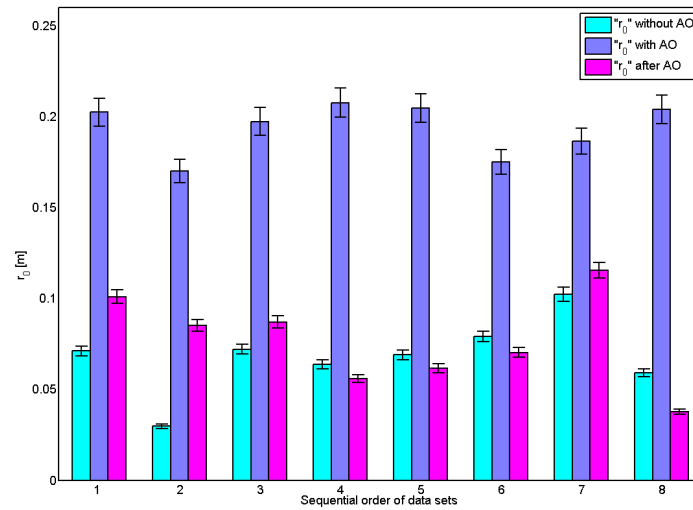
(a) Coherence length
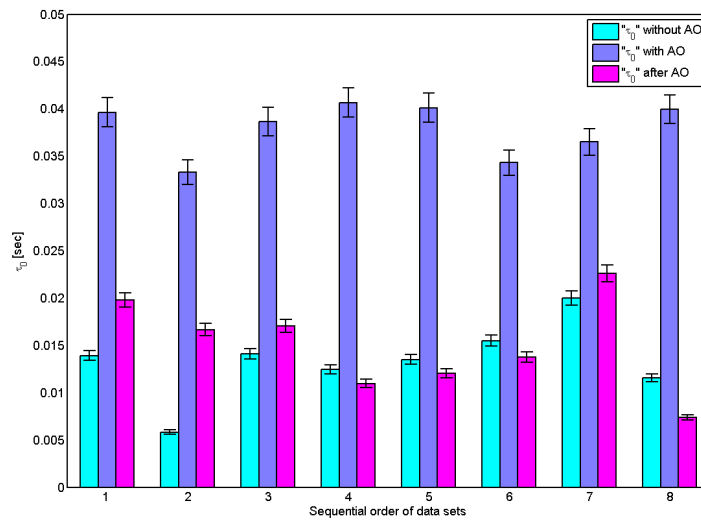
(b) Coherence time

Figure 6: Date 2010-02-24, integration time of 3 ms. Day observations.
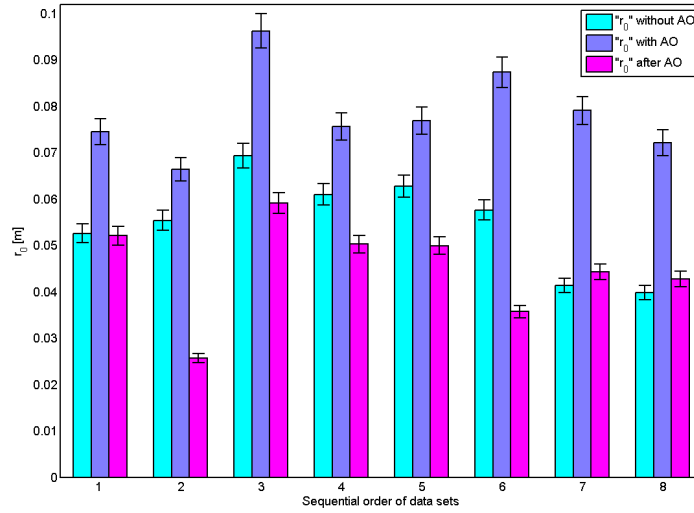
(a) Coherence length
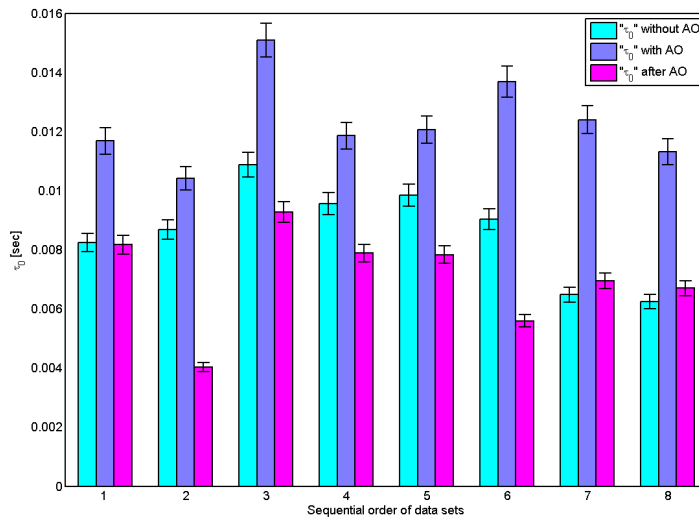
(b) Coherence time

Figure 7: Date 2010-02-28, integration time of 3 ms. Day observations.
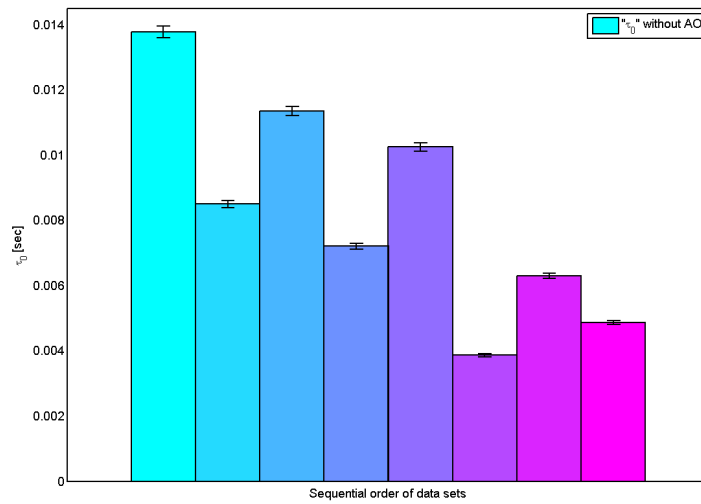
70 m, Night time:
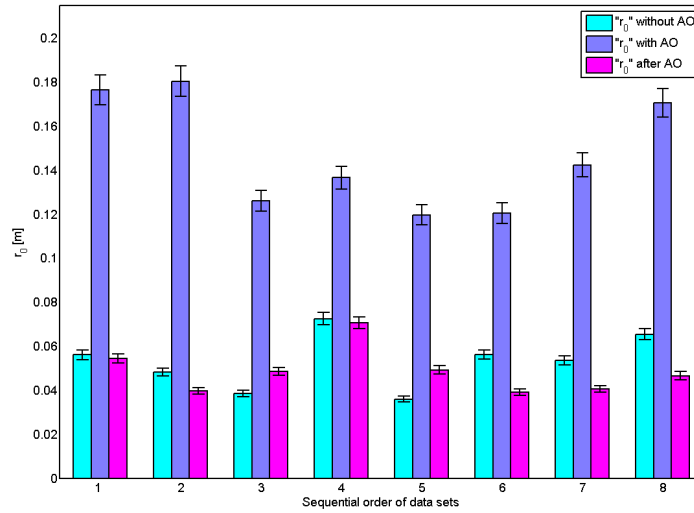
(a) Coherence length
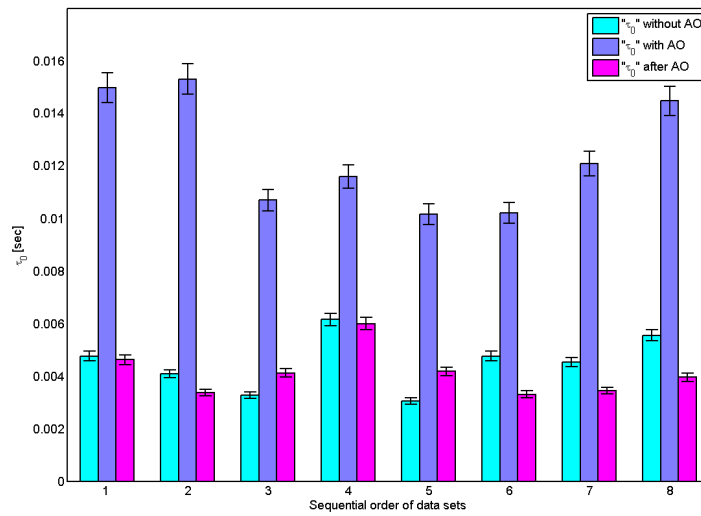
(b) Coherence time

Figure 8: Date 2010-02-24, integration time of 3 ms. Night observation.
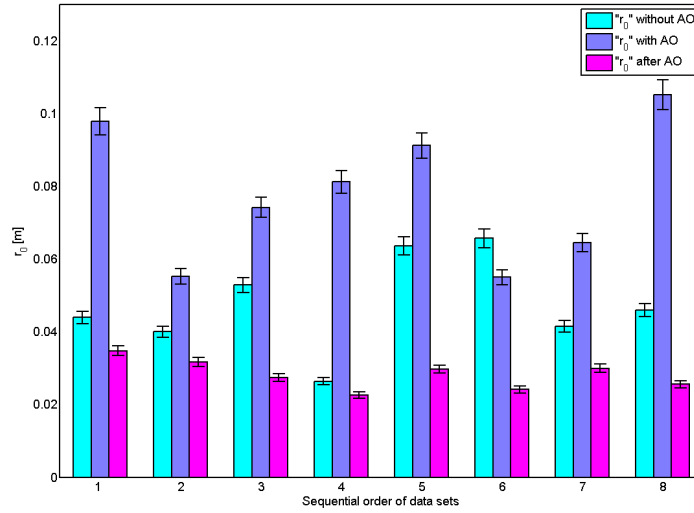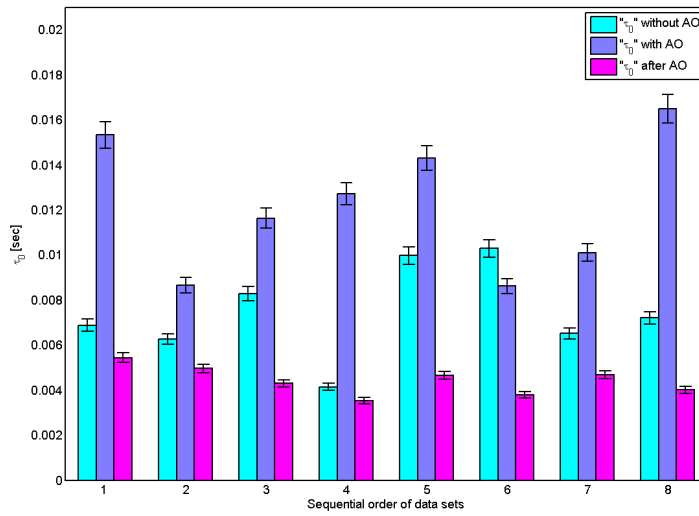
(a) Coherence length

(b) Coherence time

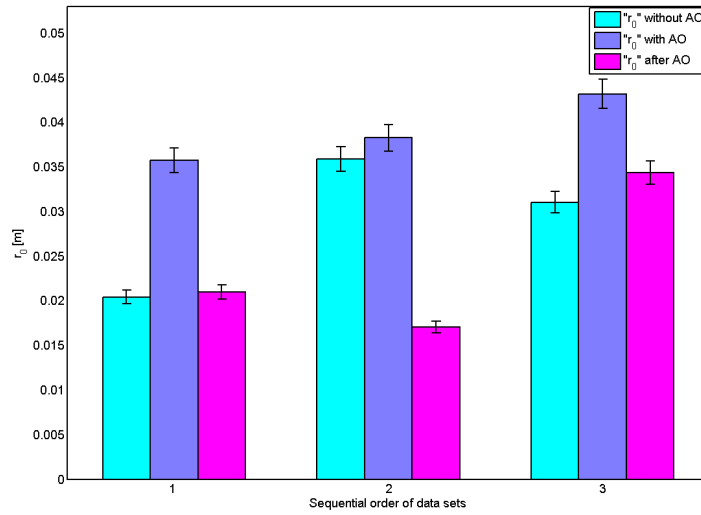Figure 9: Date 2010-03-03, integration time of 3 ms. Night observation.
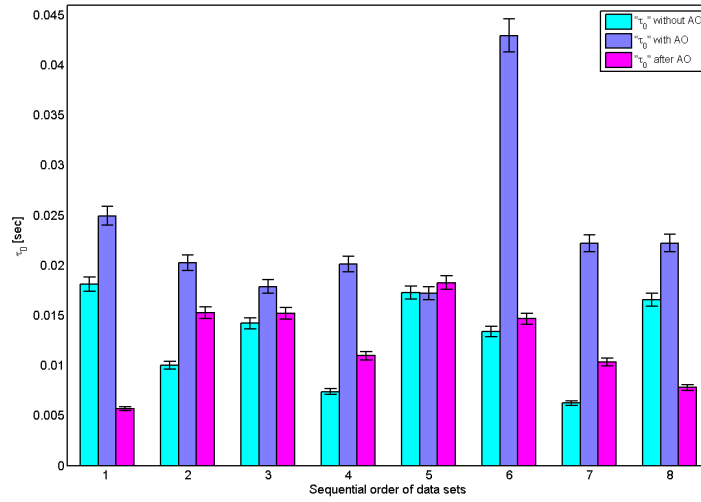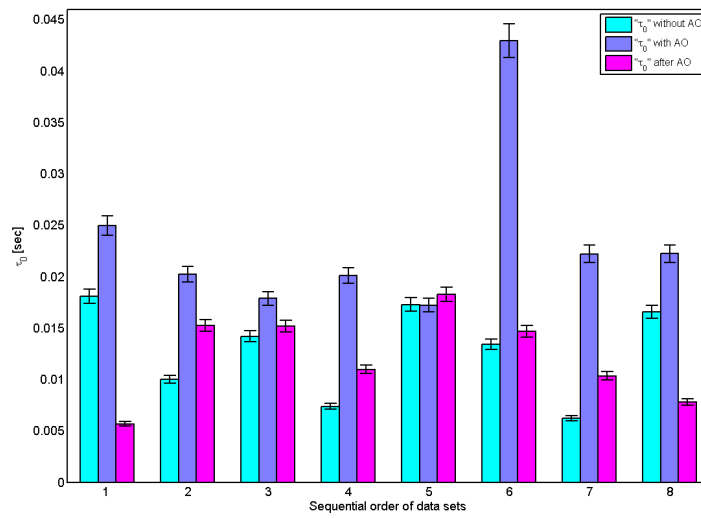
(a) Coherence length

(b) Coherence time

Figure 10: Date 2010-03-16, integration time of 3 ms. Night observation.

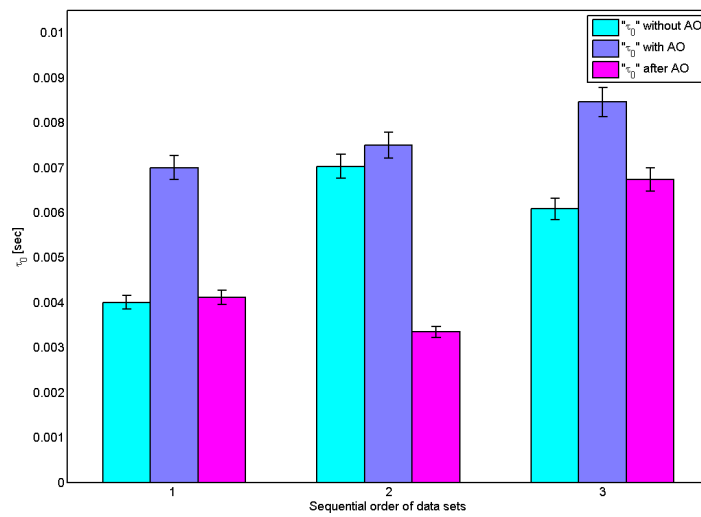**600 m**
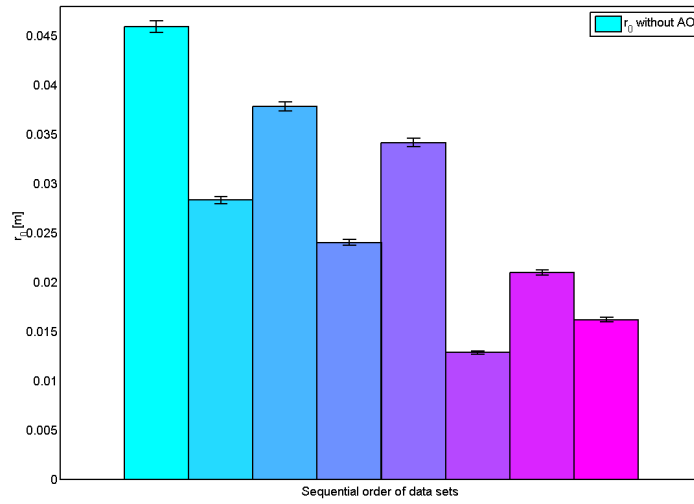
(a) Coherence length

(b) Coherence time

Figure 11: Date 2009-10-30, integration times of 1 ms for bar number 3 and 6, 5 ms for bars number 2, 4 and 7. The rest have 10 ms. Night observations.
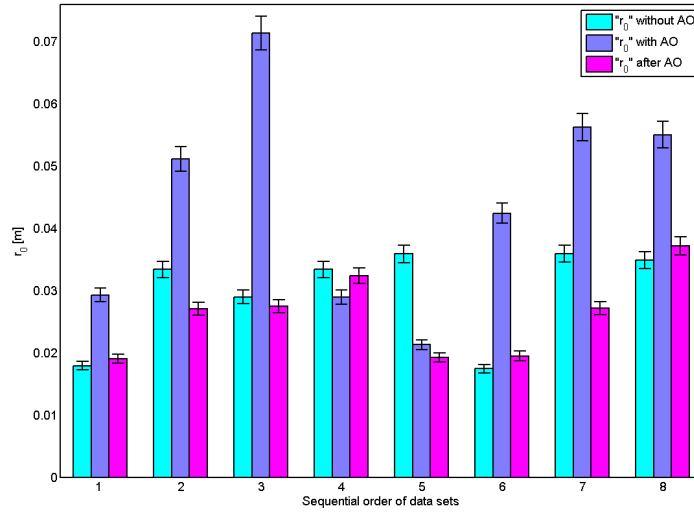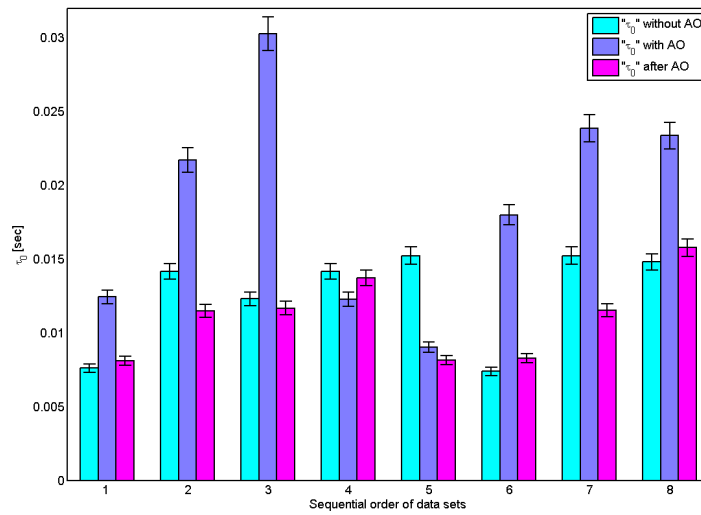
(a) Coherence length

(b) Coherence time

Figure 12: Date 2010-01-16 collection 2, integration time 5, 2 and 1 ms for bars number 1, 2 and 3. Night observation.
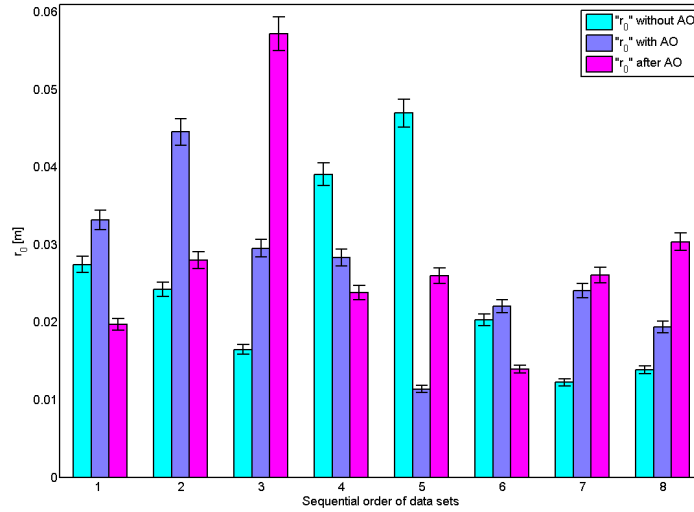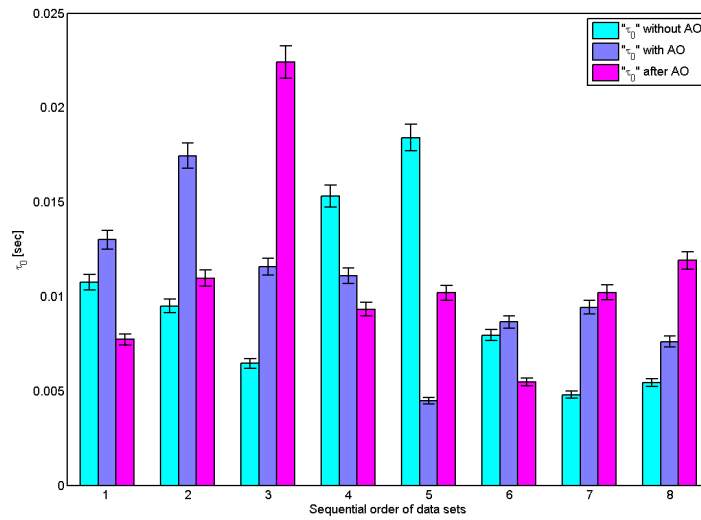
(a) Coherence length

(b) Coherence time

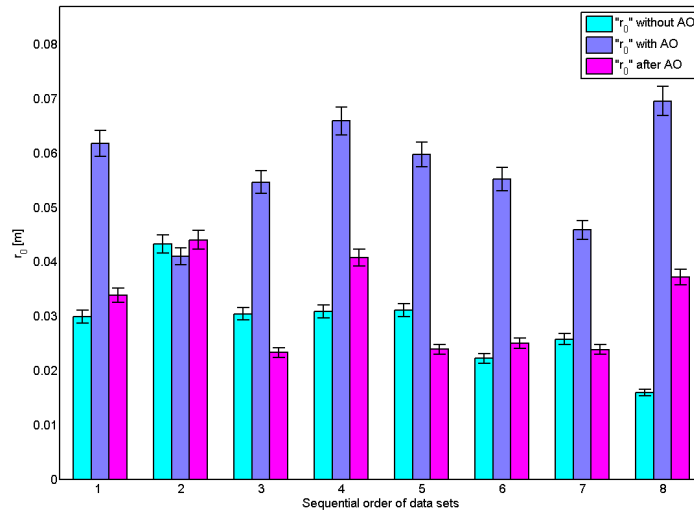Figure 13: Date 2010-01-25, integration time 3 ms. Night observation.

(a) Coherence length

(b) Coherence time

Figure 14: Date 2010-01-29, integration time 3 ms. Night observation.
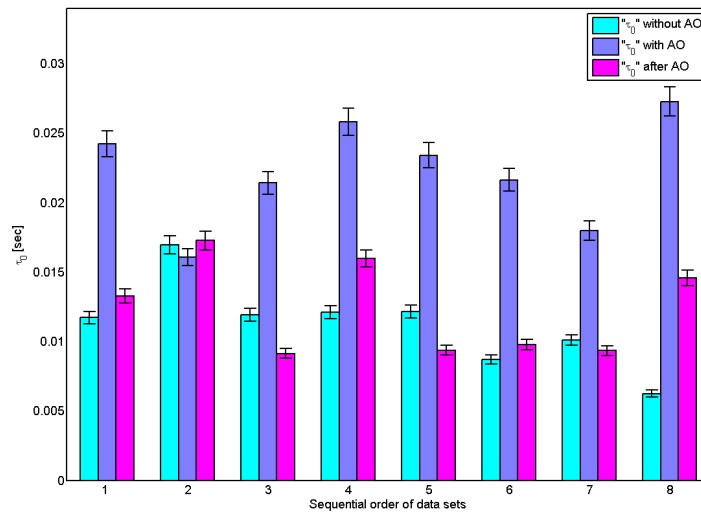
(a) Coherence length

(b) Coherence time

Figure 15: Date 2010-02-05, integration time 3 ms. Night observation.

All non "bad" sorted data

(a) r_0 before AO

(b) τ_0 before AO

Figure 14: r_0 values for "before" AO data, sorted according to "before" AO coherence lengths. t_0 values for for "before" AO data, sorted according to "before" AO coherence time.

(a) r_0 during AO

(b) τ_0 during AO

Figure 15: r_0 values for "during" AO data, sorted according to "before" AO coherence lengths. t_0 values for "during" AO data, sorted according to "before" AO coherence time.
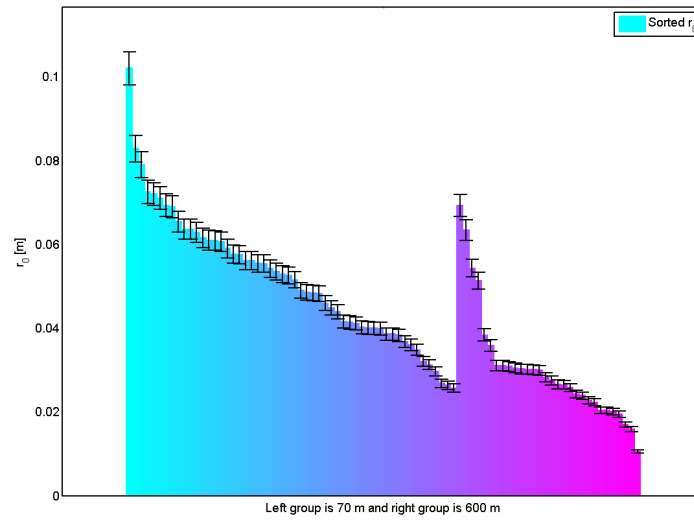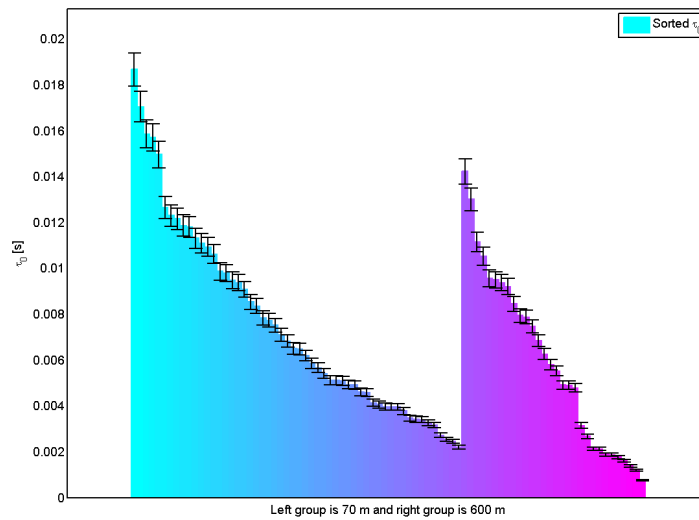
(a) r_0 after AO

(b) τ_0 after AO

Figure 16: r_0 values for "after" AO data, sorted according to "before" AO coherence lengths. t_0 values for "after" AO data, sorted according to "before" AO coherence time.
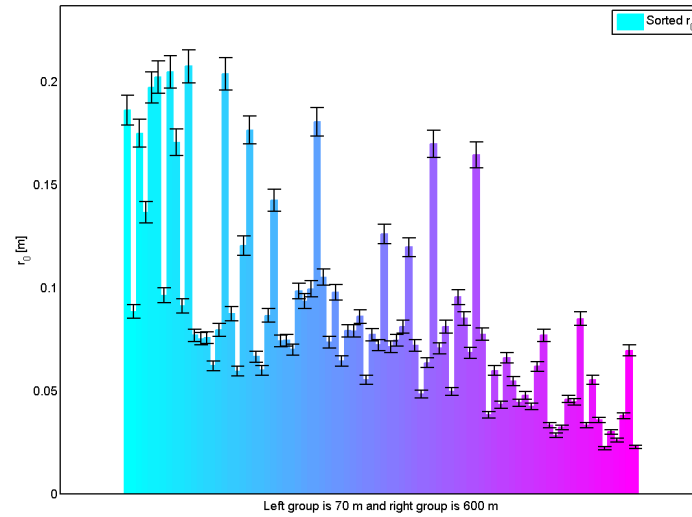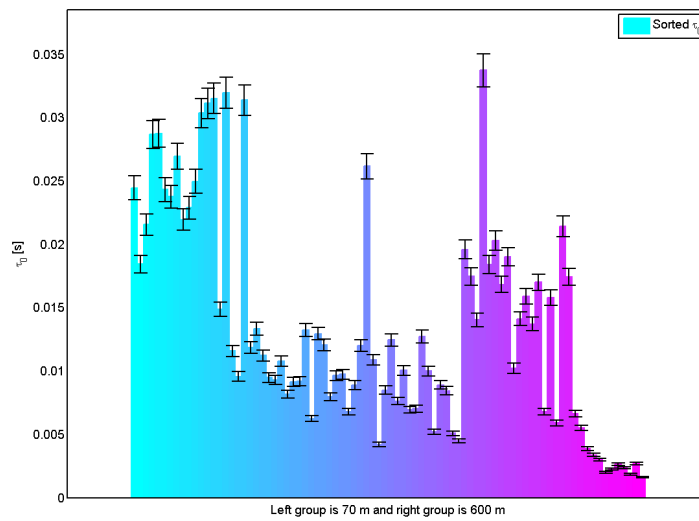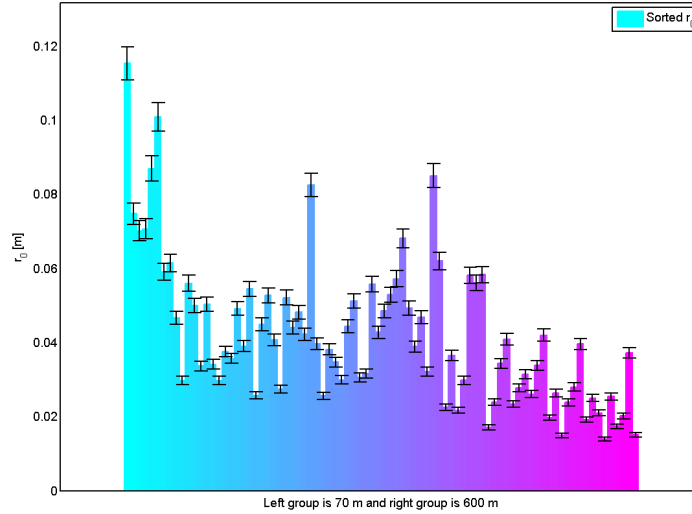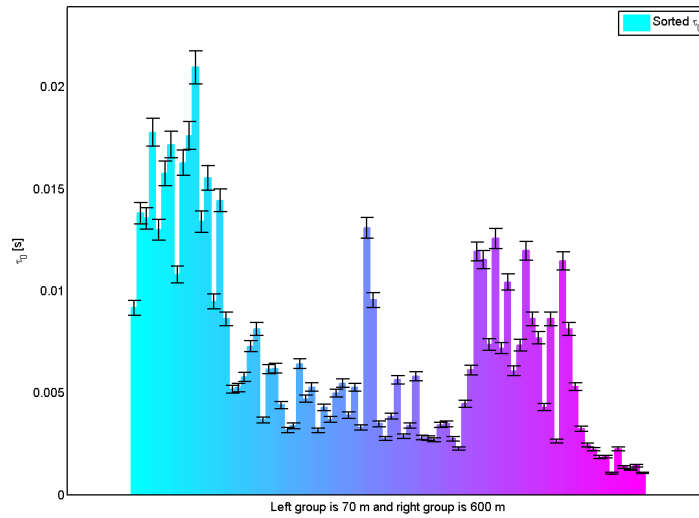
Appendix B.

Using and calibrating the Adaptive Optics setup

As mentioned in the report, this appendix is written to give an idea of how to calibrate and use the AO-setup. It is not only the direct usage of the AO-setup but rather everything that needs to be done from start to finish.

Note that there are two different calibration talked about in this appendix, the small calibration that is done when using the setup and the larger calibration that is done when the system has been moved or something has happened that affects the system in a similar way.

Using the AO-setup

Due to the greatly variable weather during the year there are two different ways of treating the AO system. During the summer the system is supposed to be turned of when not in use. During the winter however it is good to keep the computers in the dome turned on at all times so that they are both warm and so that moist do not condense on them.

For this part most of the text will be in point form with short explanations if necessary in footnotes. If there is any need for a deeper explanation the point form will be interrupted by the explanation and then continued afterwards. This part will also be split into a start up part and a shut down part. Under these parts both the AO-setup and solar telescope is explained.

Startup
AO, system

1. In the setup room turn on the power on the two extension cords in case it is summer otherwise leave them on.

2. Turn on the black expansion box (2:nd from the top in the rack), first in the back then in the front.

3. Turn the AO computer on, first in the back and then in the front in case it is summer otherwise restart this computer.

4. Start the gray DC amplifier box in the middle of the rack, first in the back then in the front.

5. Start the power supply (furthest down in the rack) and make sure that the two panels shows 15 V. If not, check the "Hardware problems and solutions" section later in this Appendix for help.

6. Adjust the currents (2:nd from the bottom in the rack) to 195 V for the left and 215 V for the right.

7. Start the image computer (the computer that is on the floor).

8. Turn on the WFS (on top of the rack).

9. Open a terminal on the AO computer (the computer that controls the AO-setup) and type:

    - cd .. $< enter >$[1]
    - cd opt/EDTpdv $< enter >$
    - ./camconfig $< enter >$

10. Check if the program just opened (camconfig) is set to "Lil Joe 80x80", if it is then press "ok", if it is not set to "Lil Joe 80x80", change it and then press "ok".

11. open a new terminal and wright:

    - cd .. $< enter >$
    - cd home/polu/linux $< enter >$
    - matlab $< enter >$

12. Check if the "current directory" set to "/home/polu/linux", otherwise change it to that one.

13. On image computer, open "Qapture Pro 6", if there is some problem look at the back of the computer to see if the usb stick with the red light is glowing[2], if not, try to correct it so that it does glow.

14. Press the camera button.

15. Press the preview button.

16. Set the "exposure time" to what is needed[3].

17. Set the "gain" to a suitable value[4].

---

[1]This means that the enter button should be pressed.
[2]This must be in place for the program to work.
[3]This is how long each image is exposed.
[4]How many times CCD detection is amplified in the output values, note that this also increases the noise.

18. Set the "contrast" to a suitable value[5].

19. Set the "offset" to a suitable value[6].

    Now that the computers are turned on and the programs are up and running, it is time to calibrate the system. NOTE that this is the normal calibration and is always needed for the setup to work properly.

20. Make sure the lights are off[7] in the room, go to the end of the setup (away from the door leading outside), lift the lid and push the reference arm into the light path, put the lid back on.

21. Turn on the test light with the generator at the end of the setup[8].

22. At the AO computer run the Matlab program "Apply bias"[9].

23. Showing on the image computer screen should now be a single light dot, if not the system needs to be calibrated more extensively (taken up later).

    The small following part is to set some parameters for the AO system to work with, this part may need to be done more than once.

24. On the AO computer, run "Aomenu".

    - Under configure:
        - Under parameters: Do not change anything.
        - Under subapertures: Each of the individual subapertures can be either enabled/disabled[10]. The number of pixels used for each subaperture can be changed and one subaperture can be set as a reference. Movement up and down, left and right can be done in steps of entire subaperture or for each subaperture at pixel length to some extent. When a suitable subaperture is chosen as reference[11] press "Save".

---

[5]Sets the contrast so that it is possible to see anything on the monitor.

[6]Sets the ground level for what is needed before the CCD output sends out information. A suitable value is 1-1.5

[7]To not overexpose the WFS or the SC.

[8]The far side to the celestron.

[9]This is to set the deformable mirrors and the tip tilt mirror in a default position so that the light goes through the setup correctly.

[10]Normally the four in the middle should be disabled because that is where the shadow of the central obstruction of the celestron should be. One to three subapertures in each corner since the celestron is circular and the WFS is quadratic the corners should get no light.

[11]One with good contrast.

- Under regions: Up to 5 guide regions for the AO-system can be set i.e. which subimages should be used as references (normally there is no need to change anything here). The size and placement can be set for each guide region. Press "Save" when done.

- Under execute:
  - Under calibrate: Have all the light in the room turned of (including the computer screens but not the WFS camera control box) and press "get bias image". Insert the reference arm in the light path and then click on the "get undistorted image".
  - Under AOmode: Here the number of SVD modes that the system uses when running the AO can be set. Press "save" when a appropriate number is chosen[12].
  - Under calibrate: This time press "Poke tip/tilt" and let that run until it is done[13]. Now press "Poke actuators" and let that run til it is done[14].

The small part that follows is to see if the AO is working properly. Look at the image computer screen when running "./mcontrol"[15]. If the results are good, be happy, do the next step in the checklist and continue your work. If the results are not good some small adjustments needs to be done, do the next step in the checklist and go back to "On the AO computer, run "Aomenu"".

25. Open a new terminal and type:

    - cd .. $< enter >$
    - cd home/polu/linux $< enter >$
    - "./mcontrol"$< enter >$
    - $< enter >$

26. Do some experiment

---

[12]This defines the number of SVD-modes the reconstructor will correct. A good number is from 3 (for tip-tilt only) to around 20.

[13]This should take a second or two. The Hartman vectors should be about a third to half the distance between the starting points for the vectors.

[14]This should take 10-15 seconds and the Hartman vectors should for each poke point to that position and should only be prominent within three or four subimages from that point.

[15]This is the command to run the AO. It will stop running when enter is pressed again.

Startup, siderostat

1. In the room that is to the right when coming up the stairs there is a rack to the right. Turn on the power to the black box that is in the bottom of the rack.

2. In the same rack, on the middle box there is a switch marked "siderostat", turn it on.

3. There is a computer that is above the box just mentioned, open the front panel and turn on the computer.

4. Go into the AO-room and on the screen without a computer (Siderostat computer, the computer that you already have turned on in the room to the right coming up from the stairs), log-in with the password.

5. On the desktop, start the "shortcut to CUI".

6. Go outside to the siderostat and remove the wind/water protection by pulling it back.

7. Remove the lids from the two siderostat mirrors.

8. On the gray wall behind the siderostat, open the lid, hinge it up.

   Depending on the experiment the third mirror can be used. If this is the case, that mirror needs to be visible by the other mirrors.

   - Go into the other dome and plug in the power cord to the dome upper door. Pull the handle to open the upper door about 30 cm, more is not needed.

   - Plug in an power extension cord and take it up to the motor that controls the lower dome door and plug the power cord into the extension power cord.

   - Open the lower dome doors as much as they can, when it does not open any more stop pressing the open button.

   - Remove the plastic bag that is over the mirror and remove the lid on the mirror. How to align this mirror is in a separate section.

9. On the Siderostat computer, in the program previously started press the arrow button in the top right and in the following pop-up press the **OUT** button[16].

---

[16]If the IN button is pressed then the big lens at the opening that leads outside will be sent up by the motors until it hits the top. Avoid this.

Depending on how the telescope is needed to be directed there are two ways to direct the siderostat, via the normal program or giving the siderostat motors commands directly.

For normal program usage:

- Press the arrow button to get the motors of the siderostat activated.

- Either select one of the targets in the selection box and press "go to object".

- If your target is not in the list, then you create one by pressing the "add new object" button and insert the correct values in the boxes.

- If you want to target the Moon, press "go to Moon".

- Additional directing is done via the "dec" or "hour" plus and minus buttons. Set the step length to appropriate length.

For direct motor control:

- Open the "Declination angle" and "Hour angle" programs.

- In the CUI program press the arrow button to get the motors of the siderostat activated.

- In both the Dec and Hour programs, be careful when inserting the wanted angles[17], not more than $\pm$ 0.6 in the Hour angle and not more than $\pm$ 2. When the values have been entered press the arrow button.

10. Turn of the test light if it is not that which is being done experiments on. Do some experiment, good luck.

---

[17]In case certain values are overstepped the siderostat needs to be recalibrated. for the hour angle this is done by going back beyond zero equal to the difference between the amount that the motors where stopped on and the maximum value, then restart the AO computer. DO NOT GO BEYOND THE BOUNDARIES IN THE DECLINATION!

Shutdown

Shutdown, AO system

1. Shut down the programs that are running. Turn of the computers if it is summer. If it is winter leave them on.

2. Turn of the WFS.

3. Turn of the test light (if it is not already done).

4. Move the reference arm (if it is not already done).

5. Lower the currents to zero (2:nd from the bottom in the rack) and turn it off.

6. Turn of the box that is lowest on the rack.

7. Turn everything starting from the top (first in the front and then in the back if needed).

8. Turn of both of the extension cords power if it is summer, otherwise leave them on.

Shutdown, siderostat

1. If you are running the motors directly; on the Siderostat computer set the Dec and Hour angles to zero and wait for them to get to zero then close the three programs and shut down the computer and monitor.

2. If you are using the normal control program; on Siderostat computer in the CUI program, press "Stop tracking" and continue down the list.

3. Press "Park telescope", wait until the declination and right assention is at 0.0, if it goes pass 0.0 press "Park telescope" again and wait, repeat until it stops at 0.0 for both.

4. Press the circle button in the top left corner to stop the motors.

5. Shut down the program, computer and monitor.

6. Go outside and close the lid on the gray wall behind the siderostat.

7. Put the lids back on the two mirrors and fasten the lids.

8. Pull the wind/water protection back over the siderostat.

If you are using the third mirror.

- Go into the other dome and put the lid on the mirror and then the plastic cover.
- Close the lower dome door and disconnect the motor from the power extension cord.
- Unplug the power extension cord from the wall.
- Close the upper dome door.

9. Go into the room that is to the right coming up the stairs, on the middle box in the rack to the right, switch off the switch marked "siderostat".

10. Turn of the power on the box in the bottom of the rack.

Calibrating the AO-setup

This part takes up the more extensive calibration needed when the setup has been lifted and lowered or when it has been tampered with in some way. It is a very time consuming process but is imperative if the setup is to work correctly. The calibration involves going back and forth between the different parts to get a final acceptable result.

To make the instructions easier to follow a table with four columns have been created. The first column contains the part name. Only the parts that have fine tuning screws on them, because the rest should not be tampered with. However moving the other parts (mainly lenses) should only change the size, focus (blurriness) and axial position of the images on the WFS and SC and also move the dots on the WFS radially away or towards the center of the dots (this center should be at the center of the "camera show" video feed). Each of the tunable parts have two screws, each of these screws have a one word description to make it clear which screw that this manual is refereeing to, i.e "Top" refers the screw that is on top of the part or physically higher up than the other screw, "Side" means the screw that is on the side of the part. "Bottom" means the screw that is physically lower down that the "Top" or "Side" screw. This is the content of column two. The third and fourth columns describes the effects in the WFS and SC screens respectively when these screws are turned clockwise as seen from the top of the screws. The effect describes what happens to the dots in the WFS and the light in the SC, how the lights move in the video feeds, i.e up and/or right. If there is no effect in either one of the WFS or the SC, that is marked with "—".

In the table L_{Ins} refers to the astigmatic lens that can be inserted into the light path just after the second deformable mirror. In this case it is the

VIII

lens that is rotated clockwise instead of a screw that is turned. The shape of the light dot also changes as it moves around in the WFS and SC when the lens is turned. Both the reference arm and the calibration arm has one tunable part each. These two are described at the bottom of the table.

Part name:	Screw descriptions	WFS screen	SC screen
DM_1	Top	Left	Down
	Bottom	Down	Right
L_7	Side	Left	Down
	Bottom	Down	Right
DM_2	Top	Right	Up
	Bottom	Down	Left
L_{Ins}	Turnable	Clockwise	Clockwise
	lens	circular motion	circular motion
Beam splitter	Top	Right	Up
	Bottom	Down	Left
WFS	Top	Left	—
	Side	Down	—
Reference arm	Top	Left	Down
	Side	Down	Left
Calibration arm	Side	Down	Left
	Bottom	Right	Up

Problem and "easy" fixes

The first thing that should be said about the programs and the computer that are running the AO-setup is that they are inherently unstable and tend to stop working from time to time for no apparent reason.

The system itself also have some problems that have not yet been solved. Some of the problems are simple to solve but when doing observations for the first time it is easy to forget even the simplest things.

The following part describes different problems that have occurred several times and gives one or two solutions to each of the problems, beginning with the software problems and then going on to the hardware problems.

Software problems and solutions

It can happen from time to time that the subaperture sub-program wont show up. The problem might be that the selected subaperture has been de-activated. This problem has two possible solutions: the first one is to go into the subaperture program code and change the selected subaperture by

changing the number on row 55. The second solution is to go into the folder "home/polu/linux/oroginal program" and copy "f.mat", then paste "f.mat" into the folder "home/polu/linux", writing over the existing file. Be careful not to do it the other way.

If the "AOmode" sub-program wont respond, restart Matlab and do a recalibration from "get bias image".

If the "Camerashow" program and the "AOmode" subprogram is active at the same time the programs will stop responding and Matlab needs to be restarted and the system re-calibrated from "get bias image" and onwards.

If the "Camerashow" program is exited without pressing the "stop" button first then the programs will stop responding and Matlab needs to be restarted and the system re-calibrated from "get bias image" and onwards.

If problems are not solved by restarting Matlab, then the simplest solution is to copy all the items in the folder "home/polu/linux/oroginal program" and paste them into the folder "home/polu/linux", writing over the existing files. Be careful not to do it the other way.

Hardware problems and solutions

If the light from the "reference arm" can not be seen in the WFS or SC then move the reference arm out and in again, it might have been slightly tilted or not pushed against the stop.

If no light from an external source can be seen in the SC or WFS when it should be visible (i.e when shining a light into the celestron to check the setup) then the mirror might not have been lifted from the "F/11" point or the monitor mirror has not been lifted.

If no light is visible in the monitor camera when it should be the monitor mirror is most likely not in place, then lower it manually.

If the monitor mirror falls out of its holder loosen the screw(s) that are in the middle on the holder sides and put in the mirror arm that is attached to the mirror into the holder hole and faster the small screw. The screws are placed in the middle hole on the left, bottom and right side of the holder. This should not be able to happen any more, but do not rule it out as a problem. When reattaching the mirror make sure that any incoming light is visible in the monitor camera so that it monitor can be used as a rough guide. Preferably so that any light or chosen area is in the FoV of the WFS and SC simultaneously as the object is in the painted square on the tape that is stuck on the monitor camera.

If the system will not start at all, then the fuse in the gray cabinet have likely gone, go to the cabinet and flip the switch fuse on.

If the reference/calibration arm lamp will not start then that fuse might

have gone. Ask the local technician for a new fuse, and a flat screwdriver to open the lamp box.

If the DM power supply does not say 15 V just wait for it to change or if it take too long (more than a minute) turn off the power supply, wait for the lights to shut down and restart the power supply. The problem is due to a safety current that goes through a small amount of liquid that changes it's resistivity. This liquid can at times be to cold and need some time to warm up.

If, for some reason, any of the connections to the deformable mirrors have become loose the power supply will fluctuate changing the shape of the mirror even when the AO system is not active. The solution to this is evident, push in the cable to the DM mirror, but be gentile so that the mirror does not move.

Easy to forget problems

If the image of the calibration arm can't be seen when trying to calibrate the setup, there can be three simple problems: the mirror in the "F/11" point has not been lowered, lower the mirror using the motor switch by switching it on. The bias might not have been applied to the deformable mirrors, in that case run the program "apply bias". The light might be blocked by the black paper that is used to shield the WFS form ambient light. Lift the paper if that is the case.